



CZECH TECHNICAL UNIVERSITY IN PRAGUE
Faculty of Nuclear Sciences and Physical Engineering
Department of Nuclear Reactors

Fission yield measurements from uranium irradiated in the VR-1 reactor

Júlia Sala Leon

Master thesis supervisor:

Dr. Jan Rataj

Academic year 2018 -2019

Czech Technical University in Prague
Faculty of Nuclear Sciences and Physical Engineering
© 2019 Júlia Sala. All rights reserved.

This thesis is school work as defined by Copyright Act of the Czech Republic. It has been submitted at Czech Technical University in Prague, Faculty of Nuclear Sciences and Physical Engineering. Without written permission of the supervisor(s) and the author(s) it is forbidden to reproduce or adapt in any form or by any means any part of this publication. Requests for obtaining the right to reproduce or utilize parts of this publication should be addressed to Czech Technical University in Prague, Faculty of Nuclear Sciences and Physical Engineering – Břehová 7, 115 19 Praha 1 – Prague (Czech Republic).

A written permission of the supervisor(s) is also required to use the methods, products, schematics and programs described in this work for industrial or commercial use, and for submitting this publication in scientific contests.

Citation of this thesis:

Sala, Júlia. *Fission yield measurements from uranium irradiated in the VR-1 reactor*. Master thesis. Czech Technical University in Prague, Faculty of Nuclear Sciences and Physical Engineering, 2019.



DECLARATION

I hereby declare that the presented thesis is my own work and that I have cited all sources of information in accordance with the Guideline for adhering to ethical principles when elaborating an academic final thesis.

I acknowledge that my thesis is subject to the rights and obligations stipulated by the Act No.121/2000 Coll., the Copyright Act, as amended, in particular that the Czech Technical University in Prague has the right to conclude a license agreement on the utilization of this thesis as school work under the provisions of Article 60(1) of the Act.

In Prague on 28th June 2019



FOREWORD

A number of people has supported and encouraged me throughout my work. Jan Rataj has been a great supervisor and his assistance has been invaluable for this thesis. I am also grateful for his support with Milan Stefanik. I am very thankful for all their help, for the time they spent correcting and teaching me and for their enthusiasm.

I am also very grateful for the help from the working personal at VR-1 reactor, without them this wouldn't have been possible. Thanks for letting me use the reactor for my thesis. I would have never been able to perform the experiment without them.

I would like to thank also my friends and family who have encouraged me a lot throughout this process. I wouldn't have done it without them.



TABLE OF CONTENTS

Declaration.....	2
Foreword.....	3
Abstract.....	6
List of figures	7
1 Introduction	9
1.1 Motivation and goals	10
2 Theoretical background.....	12
2.1 Fission.....	12
2.1.1 Fission yields applications.....	14
2.2 Basic nuclear physics.....	15
2.2.1 Radioactive decay.....	15
2.2.2 Kinetics of Decay of Radioactive Nuclides.....	17
2.3 Neutron activation analysis.....	18
2.3.1 Introduction	18
2.3.2 Neutron source.....	22
2.4 Gamma Ray Spectrometer	23
2.4.1 HPGe detector	24
2.4.2 High voltage power supply.....	28
2.4.3 Amplifier	28
2.4.4 Analogue to Digital Converter (ADC)	28
2.4.5 Multi-Channel Analyzer (MCA)	29
2.5 Spectrum formation	29
2.5.1 Origin of X and γ radiation.....	29
2.5.2 Photon interaction with matter	30
2.5.3 Pulse height spectrum.....	34
2.5.4 Energy transferred to the detector	35



2.5.5	Spectrum components	35
2.5.6	Background.....	37
3	Methodology	40
3.1	Preparation of the sample.....	40
3.2	Irradiation.....	41
3.3	Measurements	42
4	Results	44
4.1	Results of the first measurement.....	48
4.2	Results of the second measurement	50
4.3	Results of the third measurement.....	52
4.4	Results of the fourth measurement	54
5	Discussion	55
5.1	Reaction rate for fission	55
5.2	Reaction rate for fission and reaction rate for neutron capture.....	55
5.3	Comparison with results from MCNP	56
6	Conclusion.....	58
7	References	60
	Appendix 1: Nuclide library	61
	Appendix 2: Gamma-spectrometry results	63
	Measurement 1	63
	Measurement 2.....	67
	Measurement 3.....	74
	Measurement 4.....	85



ABSTRACT

This master thesis gives the theoretical description and practical measurement of fission yields from a sample of depleted uranium irradiated for 15 minutes in a research reactor, i.e. VR-1 reactor of the CTU in Prague. First, a theoretical background is given so that the results can be understood. This theoretical background consists on the description of the fission process itself and the applications of fission yields. Also, some basic nuclear physics will be described. Specifically, radioactive decay and its kinetics will be covered. The present work also includes an explanation about Neutron Activation Analysis, what it is and what was the neutron source used. Then, the gamma ray spectrometer is described, covering all its components: HPGe detector, high voltage power supply, amplifier, ADC and MCA. To understand the results obtained using this gamma ray spectrometer, an explanation of the spectrum formation is also included in this thesis. Then, one can find the methodology that was used, and the results obtained. The discussion covers: the reaction rate for fission obtained in every measurement, the comparison of the reaction rate for fission with the reaction rate for neutron capture obtained and a comparison of these reaction rates with other studies performed in the same laboratory in similar conditions.



LIST OF FIGURES

Figure 1: Components of the binding energy per nucleon based on the semi-empirical mass formula; from [1].	12
Figure 2: Critical energies for fission in MeV; from [1].	13
Figure 3: Schematic layout of a fast transfer pneumatic system for INAA, (1) Reactor; (2) Gamma-spectrometer; (3) Valves; (4) Sample changer; from [3].	23
Figure 4: Block diagram of a basic gamma spectrometry system; from [7]	23
Figure 5: Typical Gamma ray Spectrum output visualized on a computer; from [7]	24
Figure 6: Different types of detectors; from [5]	24
Figure 7: Example of a full-energy peak efficiency curve for germanium detector; from [7].	26
Figure 8: Two HPGe coaxial detectors of different sizes. The one to the left has a relative efficiency of 80%, the one to the right only 35%; from [7]	26
Figure 9: spectra collected using germanium (HPGe); from [7].	28
Figure 10: Typical HV power supply; from [5]	28
Figure 11: Typical amplifier; from [5]	28
Figure 12: Electromagnetic spectrum; from [7].	29
Figure 13: Probability of the photoelectric effect; from [7]	31
Figure 14: Compton effect; from [7].	31
Figure 15: Train of pulses delivered at the output detector; from [7]	34
Figure 16: Pulse height spectrum; from [7].	34
Figure 17: Components of Spectrum; from [7].	36
Figure 18: Full energy event; from [7].	36
Figure 19: Full energy peak (FEP); from [7].	36
Figure 20: Scattered gamma-rays escape from the detector; from [7].	37
Figure 21: Compton edge and continuum; from [7].	37
Figure 22: A low-background shield configuration for a germanium detector; from [8].	39
Figure 23: Background spectrum recorded for a Ge detector using the shielding shown on Figure 22; from [8].	39
Figure 24: Sample of depleted uranium being cut at the left and final shape of the sample at the right.	40
Figure 25: Weighing procedure.	40



Figure 26: Sample in the plastic capsule.	41
Figure 27: Pneumatic system. Terminal at the laboratory at the left side and terminal at the reactor to the right.....	41
Figure 28: Operating conditions of the reactor.....	42



1 INTRODUCTION

Neutron activation analysis (NAA) is a method for qualitative and quantitative determination of elements based on the measurement of characteristic radiation from radionuclides formed directly or indirectly by neutron irradiation of the material. The most suitable source of neutrons is usually a nuclear research reactor. The method's characteristics can be summarized as follows:

- (1) Very low detection limits for 30–40 elements,
- (2) Significant matrix independence,
- (3) The possibility of non-destructive analysis (instrumental NAA or INAA),
- (4) The use of radiochemical separation to overcome interference in complex gamma-ray spectra (radiochemical NAA or RNAA),
- (5) An inherent capability for high levels of accuracy compared to other trace element analysis techniques.

On the other hand, *gamma ray spectrometry* is an analytical method that allows the identification and quantification of gamma emitting isotopes in a variety of matrices. In one single measurement and with little sample preparation, gamma ray spectrometry allows you to detect several gamma-emitting radionuclides in the sample. The measurement gives a spectrum of lines, the amplitude of which is proportional to the activity of the radionuclide and its position on the horizontal axis gives an idea on its energy.

Applications of gamma ray spectrometry include:

- monitoring in nuclear facilities,
- health physics,
- nuclear medicine,
- research in materials,
- bioscience,
- environmental science, and
- industrial uses of radioisotopes.

A conservative estimate is that over 200,000 gamma-ray spectrometers are in use in academic and industrial labs and facilities throughout the world. Because of the highly technical nature of this technique, the training of scientists and engineers in this area has been a continuing challenge.



Regarding *fission yields*, sets of evaluated yields are of importance for a large community of people because fission yields have an impact on different fields of interest.

From a theoretical standpoint they are interesting for the understanding of matter, because they allow the description of the phenomena occurring in a nucleus undergoing large collective motion at low excitation energy and, hence, are influenced by nuclear shells that disappear at higher excitation energies.

From a practical standpoint fission yields are of importance for the design of nuclear reactors and for waste management. The design of alternative reactors may be crucial for the future energy supply of mankind. The yields of "delayed neutron precursors" and their neutron emission probability (P_n -values) determine reactor dynamics and, hence, the safety of a reactor against prompt criticality. The inventory of fission products in a reactor and their decay characteristics determine the possible hazard of contamination in the case of an accident. They also determine the amount of heat produced by a reactor core after shut-down and in consequence the amount of emergency cooling that must be foreseen. The inventory and the neutron absorption cross sections of the fission products finally determine the neutron economy in a reactor and its possibilities in neutron induced reactions (like incineration of actinides and fission products).

In consequence, the measurements of fission yields have started right after the discovery of nuclear fission and are continuing, thus involving a large number of scientists and a large variety of experimental methods.

1.1 MOTIVATION AND GOALS

Over the past fifty years, research reactors have progressed through a variety of tasks. These have included materials research using neutron scattering and diffraction, materials characterization by activation analysis and radiography, isotope production, irradiation testing, as well as training, and service as centers of excellence in science and technology. Despite these efforts, research reactors in some countries are still under-utilized. This is especially true in the 39 developing countries which together have 84 operational research reactors. Since research reactors have a high capital cost and require a substantial operating budget, seems fair to work on their effective utilization.

Due to its inherent sensitivity and accuracy, neutron activation analysis (NAA) has been extensively applied to environmental sciences, nutritional studies, health related studies,



geological and geochemical sciences, material sciences, archaeological studies, forensic studies and nuclear data measurements. In addition to these applications, NAA has a role in the quality assurance of chemical analysis. Since NAA requires access to a nuclear research reactor, the method is less widely applied than other analytical techniques for elemental analysis, such as atomic absorption spectroscopy (AAS), inductively coupled plasma spectroscopy (ICP) and X-ray fluorescence spectroscopy (XRF). These are all techniques for which stand-alone equipment is easily available and consequently, the call on NAA for elemental analysis is decreasing. Thus, also the utilization of the reactor is also affected.

The decreased interest for NAA results partly from insufficient awareness within the applied fields regarding the opportunities of this technique. Each analytical technique has its own particular advantages and disadvantages that make it suitable (or unsuitable) for a given application. NAA is unique in several important aspects such as being largely independent of matrix effects, being suitable for analysis of materials that are difficult to dissolve (e.g. silicon, ceramics), being relatively insensitive to sample contamination and having specific means of detection. Due to these comparative advantages, sensitivity and accuracy, it has a special role as a reference technique for other analytical methods.

So, the motive of and the subject for writing the present study comes from the opportunity to be able to both use a research reactor, and so contribute to their effective utilization, and also use NAA and contribute to increase the awareness about the topic.

Regarding the goals of the present thesis, four main goals can be stated:

1. Study fission process of uranium.
2. Study products that come from this fission process.
3. Study a neutron activation analysis and neutron activation technique using dosimetry foils
4. Utilization of this method for the measurement of fission product yields from uranium irradiated by neutrons.



2 THEORETICAL BACKGROUND

2.1 FISSION

Neutrons colliding with certain nuclei may cause the nucleus to split apart – to undergo *fission*. This reaction is the principal source of nuclear energy for practical applications.

Binding energies of nuclei per nucleon decrease with increasing atomic mass number, for A greater than about 50. This means that a more stable configuration of nucleon is obtained whenever a heavy nucleus splits in two parts – that is undergoes fission. The heavier, more unstable nuclei might therefore be expected to fission spontaneously without external intervention. Such fissions do occur.

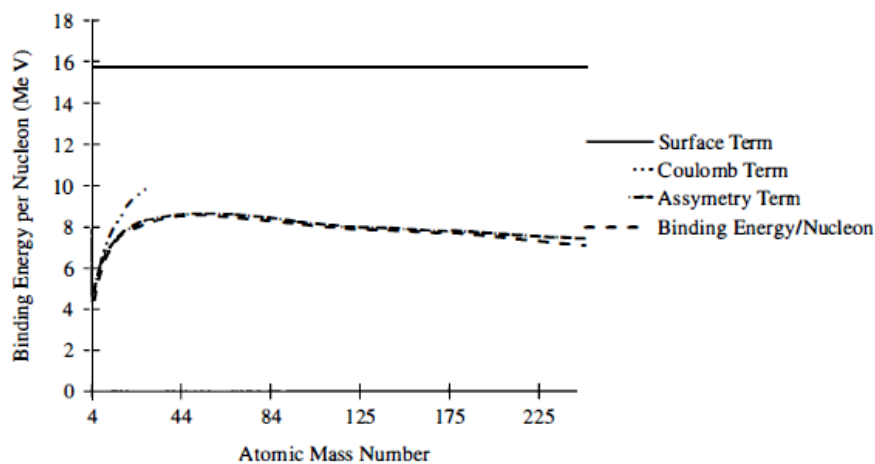


Figure 1: Components of the binding energy per nucleon based on the semi-empirical mass formula; from [1].

Figure 1 shows the terms in the binding energy per nucleon curve as determined from the liquid drop model of the atom. The decrease in binding energy per nucleon is largely due to the coulomb term overcoming the volume term. The volume term represents the binding due to the strong nuclear forces. It is the coulomb repulsion, then, that is largely responsible for fission.

Although heavy nuclei do spontaneously fission, they do so only rarely. For fission to occur rapidly enough to be useful in nuclear reactors, it is necessary to supply energy to the nucleus. This, in turn, is due to the fact that there are attractive forces acting between the nucleons in a nucleus, and energy is required to deform the nucleus to a point where the system can begin to split in two. This energy is called the *critical energy of fission* and is denoted by E_{crit} . Values of E_{crit} are given in Figure 2 for several nuclei.



Fissioning Nucleus A_Z	Critical Energy	Binding Energy of Last Neutron in A_Z
^{232}Th	5.9	*
^{233}Th	6.5	5.1
^{233}U	5.5	*
^{234}U	4.6	6.6
^{235}U	5.75	*
^{236}U	5.3	6.4
^{238}U	5.85	*
^{239}U	5.5	4.9
^{239}Pu	5.5	*
^{240}Pu	4.0	6.4

*Neutron binding energies are not relevant for these nuclei since they cannot be formed by the absorption of neutrons by the nuclei $^{A-1}_Z$.

Figure 2: Critical energies for fission in MeV; from [1].

Any method by which energy E_{crit} is introduced into a nucleus, thereby causing it to fission, is said to have *induced* the fission. The most important of these is the neutron absorption. When a neutron is absorbed the resulting compound nucleus is formed in an excited state at an energy equal to the kinetic energy of the incident neutron plus the separation energy or binding energy of the neutron in the compound nucleus. If this binding energy alone is greater than the critical energy for fission of the compound nucleus, then fission can occur with neutrons having essentially no kinetic energy. For example, according to Figure 2, the binding energy of the last neutron in ^{236}U is 6.4 MeV, whereas E_{crit} is only 5.3 MeV. Thus, when a neutron of zero kinetic energy is absorbed by ^{235}U , the compound nucleus, ^{236}U , is produced with 1.1 MeV more energy than its critical energy, and fission can immediately occur. Nuclei such as ^{235}U , that lead to fission following the absorption of a zero-energy neutron, are called *fissile*. Note, however, that although it is the ^{235}U that is said to be fissile, the nucleus that actually fissions in this case is the ^{236}U .

With most heavy nuclei other than ^{233}U , ^{235}U , ^{239}Pu and ^{241}Pu , the binding energy of the incident neutron is not sufficient to supply the compound nucleus with the critical energy, and the neutron must have some kinetic energy to induce fission. In particular, this is always the case when the struck nucleus contains an even number of nucleons since the binding energy of the incident neutron to an even-A nucleus is always less than to an odd-A nucleus. For instance, the binding energy of the last neutron in ^{239}U is only 4.9 MeV, and this is the excitation of the compound nucleus formed when a neutron of zero kinetic energy is absorbed by ^{238}U . Since E_{crit} for ^{239}U is 5.5 MeV, it is clear that fission cannot occur unless the neutron incident on the ^{238}U has an energy greater than about 0.6



MeV. Nuclei such as ^{238}U , which do not fission unless struck by an energetic neutron, are said to be *fissionable but nonfissile*.

2.1.1 Fission yields applications

One can distinguish two main areas of the use of fission yields: in fundamental physics, their significance lies in all aspects of the probability of fragment formation in the fission process, whereas in applied user fields they are needed for calculating the accumulation and inventory of fission products at various stages of the nuclear fuel cycle.

Here the most important application fields and their fission yield requirements are briefly summarized:

In *reactor design and operation*, fission yields are used in criticality and reactivity calculations, for fuel and reactor core management, for reactor safety (including fission product gas production and release, fuel failure detection and contamination of reactor components) and in determining limits of safe operation in new plants and for nuclear materials transport. *Burnup* determination and *decay heat* calculations are treated separately as special cases. Generally, the required accuracies are met by existing data. It should be noted that for the various reactor types, fission yields should be known as function of incident neutron energy. For contamination and gas production detection, ternary fission yields (tritium, helium) are needed.

For the *reprocessing of spent fuel* and the *management of nuclear waste* (temporary spent fuel storage and final waste depositories) it is important to know the fission products present primarily as a source of radiation (heat production and potential hazard to the environment and personnel). Fission yields enter calculations of fission product inventory and radioactivity (*decay heat*).

The *burnup* is a measure of the total number of fission events that have occurred in nuclear fuel and hence of the consumption of fissionable material. The burnup is predicted by reactor calculations and experimentally determined for actual spent fuel with the purpose of allowing an accurate evaluation of the fuel and reactor performance. For certain methods, fission products are used as burnup monitors and their fission yields are required with high accuracy for the evaluation of measurement results.

Two types of fission product *decay heat* can be distinguished:



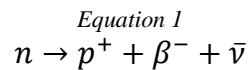
- The *residual heat after reactor shutdown* is due to radiation emitted by fission products and actinides present in nuclear fuel in the reactor core and is most important in the event of a loss-of-coolant accident. Its accurate knowledge, especially in the time from 1 to 1000 seconds after reactor shutdown, is crucial for the dimensioning of the maximum reactor power and the emergency cooling system. The fission product decay heat is obtained by summation calculations that include all contributing fission products (short lived, with half-lives longer than a few tenth of a second) with their fission yields (and decay data).
- The *decay heat from spent fuel* is due to radiation emitted by (well known) long lived fission products (and actinides). Its significance is outlined above (waste).

In nuclear materials *safeguards*, certain methods for *spent fuel assay* use fission yields (and other nuclear data) of monitor fission products for the verification (by measurement and/or calculation) of statements by reactor operators [2].

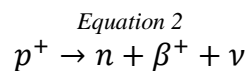
2.2 BASIC NUCLEAR PHYSICS

2.2.1 Radioactive decay

Most radioactive decays occur via the transformations ‘neutron \rightarrow proton’ and ‘proton \rightarrow neutron’ are called β -decays. They are characterized by the mass number, ΔA , which remains unchanged, whereas the atomic number is changed by ± 1 . There are three transformations of this type. A neutron is transformed into a proton by a β^- process:



The proton remains in the nucleus, whereas the electron (β^-) and the antineutrino ($\bar{\nu}$) are emitted from the nucleus, with high kinetic energies. The electron is written as β^- and not e^- , to show that it is not an atomic electron. A proton can be transformed into a neutron by two processes. One process is β^+ decay, in which a proton is transformed into a neutron and a positron ($\beta^+ = e^+$), an entity similar in mass to an electron but which has an opposite charge:



In this process there is also an emission of a neutrino (ν). Another process is the reaction of a proton with one of the surrounding electrons in the atom to yield a neutron. This process is called electron capture (EC). The neutrino and antineutrino are very small



particles with no charge, and consequently they are very difficult to detect. They are not important in the activation analysis except for their effect on the β energies.

Most radionuclides are not pure β emitters, but they emit simultaneously also a γ -photon (more accurately, the γ emission occurs in a very short time of $<10^{-10}$ s after the β^- emission). γ -Rays are electromagnetic waves, like light and radio waves, but they have much higher energies (much shorter wavelengths). They have usually higher energies than X-rays, although the main difference between X-rays and γ -rays is their sources. X-rays are due to atomic transitions (transitions between different energy levels of electrons), whereas γ -rays are due to nuclear transitions (transitions between different energy levels of the nucleons). In most cases β^- decay does not yield the ground state of the product nuclide but forms it in an excited state. The excited-state nuclide decays very rapidly (in most cases) to the ground state by the emission of either γ -rays or atomic electrons called conversion electrons. The emitted conversion electrons have no importance in activation analysis and we can neglect their emission and refer only to the emission of γ -rays.

A very important difference between β processes and γ decay (besides the difference in entities of the emitted particles, electrons vs photons, and the difference in ΔA , ± 1 in the β process and 0 in the γ decay) is the fact that in β processes. The importance of this difference lies in the fact that each nuclear decay is a transformation between two discrete energy states, resulting in a definite energy released in the process. If only one particle is emitted from the nucleus, this particle has a defined energy. When two particles are emitted, the released energy is distributed between them, and each particle can have a spectrum of energies ranging from zero up to a maximum energy, equal to the released energy. Since the emitted γ -photons have definite energies, they can be used in order to identify their emitters, by the measurement of the energy of the photons. As β -particles do not have definite energies, they usually cannot be used to identify their emitters.

In Instrumental Neutron Activation Analysis (INAA), we need to identify the different radionuclides (in order to know the nuclide from which they were formed), in addition to the measurement of their activities. This is the reason why INAA employs almost exclusively the measurement of the spectrum of emitted γ -photons. In a few cases, where the indicator radionuclide (IRN) is a pure β^- emitter, it can be measured only in cases where there are only few (2-3) nonspecific γ -emitter IRNs in the sample with different



half-lives. Their separate activities can be measured by measuring the activities at different times (measuring the decay curve) and extracting the various activities from the time dependence of the measured activity.

We said that the γ -photons emitted are due to the de-excitation of the nuclide produced in the β process. However, this de-excitation does not always have to be by only one photon. Moreover, not all β decays lead to the same level of excitation these two facts together with the de-excitation by emission of conversion electrons (mainly from low-lying levels) lead to the possibilities that one radionuclide can have more than one kind (energy) of photon and that the number of photons should not be equal to the number of nuclides which have decayed (disintegrated). The number of photons of specific energy emitted per 100 disintegrated nuclides is called the *intensity* of the γ line, expressed as a percentage.

2.2.2 Kinetics of Decay of Radioactive Nuclides

The decay of radioactive nuclides is statistical process. Thus, the number of atoms decaying per unit time (rate of decay) is proportional to the number of atoms of that specific radionuclide present in the sample. If the number of nuclei (atoms) of a specific radionuclide at time t is N^* , their rate of disappearance (decay or disintegration) is given by Equation:

$$\text{Equation 3} \\ -\frac{dN^*}{dt} = \lambda N^*$$

The constant λ , which is different for each radionuclide is called the *decay constant* of this radionuclide. Integration of the Equation 3 leads to the decay equation of radionuclides, i.e. the equation describing the time dependence of the number of atoms of the specific radionuclide:

$$\text{Equation 4} \\ N^*(t) = N_0^* e^{-\lambda t}$$

where N_0^* is the number of atoms at time chosen as $t = 0$. This formula indicates the existence of a constant lifetime for the half of the atoms, which is called the *half-life*. It means that independently of the value of N_0^* , it takes the same time (for a specific radionuclide) for disintegration of half of the atoms leaving only $N_0^*/2$ atoms of that radionuclide. For example, if the half-life is $t_{1/2} = 2.5$ days, we know that after 2.5 days only half of the original atoms remain, and after 5 days the number of original atoms is



reduced to one quarter. Substituting $N^*(t)$ by $N_0^*/2$ in the *Equation 4* leads to the correlation between the half-life ($t_{1/2}$) and the decay constant (λ) [3]:

$$t_{1/2} = \frac{\overset{\text{Equation 5}}{\ln 2}}{\lambda} = \frac{0,693}{\lambda}$$

2.3 NEUTRON ACTIVATION ANALYSIS

2.3.1 Introduction

Activation analysis is a method of quantitative chemical analysis based on the nuclear activation of the chemical elements present in the analyzed samples. It relies on the nuclear reaction between projectiles and target nuclei. The method is one of the most sensitive methods of chemical analysis. The discovery of nuclear activation, i.e., the reaction of elements with other nuclei or subnuclei particles to give radioactive substances, was made in 1934 by Irene Joliot Curie and Frederic Joliot who bombarded aluminum, boron and magnesium with naturally occurring alpha particles. The suggestion to use the activation method for elemental analysis was done in 1936 by Hevesy and Levi who used neutrons as the bombarding projectiles to activate dysprosium and europium. The method could be used either if newly produced nuclei were radioactive with appropriate half-lives and emitted radiation (by measurement of this delayed radiation) or even if the newly produced nuclide was stable or had undesired radiation or half-life by the measurement of the radiation (photons or small particles) emitted in the time of activation – a prompt radiation measurement. The use of delayed measurement is the more common one [4].

Neutron activation analysis (NAA) is an analytical technique based on the measurement of characteristic radiation from radionuclides formed directly or indirectly by neutron irradiation of the material of interest. In the last three decades, neutron activation analysis has been found to be extremely useful in the determination of trace and minor elements in many disciplines. These include environmental analysis applications, nutritional and health related studies, geological as well as material sciences. The most suitable source of neutrons for NAA is a research reactor [5].

The amount of emitted radiation depends on the number of atoms which have been activated and this number is proportional to the number of atoms in the target sample.



Consequently, activation method can be used to analyze quantitatively the elemental contents of the sample [4].

The rate of nuclear reaction in a given irradiation system is proportional to the flux of the incident radiation and the number of the target nuclei. The proportionality constant depends on the probability that an incident particle will react with a target nucleus. This probability expressed in terms of area is called the *cross-section* σ of a particular reaction. Besides these factors (flux projectiles, number of target nuclei, an activation cross-section), the induced activity depends on the duration of the irradiation and the half-life of the formed radionuclide.

The nuclear activation of the analyzed samples is followed by the quantitative detection (counting of radioactive emission) and identification of the induced activity as to the type of radiation emitted, its energy, and its half-life. The most common and sensitive method of activation analysis is by activation with *thermal neutrons* in the high flux of a research reactor and measuring the radioactivity induced in the newly formed radionuclides from the stable isotopes present in the sample [4]. The nuclear reactor is the most important source for bombarding particles for determination of trace elements by activation analysis due to its relatively high flux of bombarding particles and the relatively high cross-sections for the radiative capture reaction of thermal neutrons (n, γ) [6].

The irradiated samples usually contain more than one element which becomes radioactive and hence the accuracy and the sensitivity of the analysis are often dependent on the ability to distinguish between the radiation of the different radioisotopes or to separate the different elements in the irradiated mixture. If a complete separation of the elements is done, their radioactive emission can be measured very accurately with simple instrumentation. However, this method requires a lot of chemical work and this method is almost neglected in most cases and a purely *instrumental activation analysis* (IAA) is used or at least the separation of the mixtures to small number of fractions in which several elements are measured simultaneously.

The purely IAA has the following advantages:

1. Multielement determination in one measurement,
2. Lower costs of analysis although it requires more expensive equipment for measurement,
3. Ease automation,



4. Ability to use short-lived radioisotopes which for some elements are the only ones available,
5. Being nondestructive and being able to be used for precious samples or those which do not dissolve easily,
6. No question of efficiency of the separation process and the errors due to this process are involved.

Activation analyses are done mainly with the measurement of gamma rays due to their high penetration (in contrast to charged particles and X-ray photons), the large number of elements which produce gamma-emitting nuclides, and the existence of high-resolution gamma-ray spectrometers which allow the determination of the energy of the gamma rays. The different radionuclides produced in activation analysis are distinguished by their different gamma-ray energies and sometimes also by their half-lives [4].

Chemical analysis by nuclear activation is an *elemental analysis*, i.e. it determines the contents of the various elements in the analyte sample, but cannot tell in what chemical form (compounds, valence states, etc.) they are present. The analysis is based on a reaction of the analyte element with nuclear projectiles (neutrons, accelerated small charged particles, e.g. protons, or γ -photons):



Equation 6

In *instrumental neutron activation analysis* (INAA) the projectile is a thermal neutron and the measurement of the concentration of the element is done via the heavy product, if it is a radionuclide which emits γ -rays. As previously stated, the amount produced of the radionuclide is proportional to the number of the target atoms [3].

Due to its inherent sensitivity and accuracy, neutron activation analysis has been extensively applied to environmental sciences, nutritional studies, health related studies, geological and geochemical sciences, material sciences, archaeological studies, forensic studies and nuclear data measurements. In addition to these applications, NAA has a role in the quality assurance of chemical analysis [5].

It is hardly possible to provide a complete survey of current NAA applications; however, some trends can be identified. At specialized institutions, NAA is widely used for analysis of samples within environmental specimen banking programs [5]. Additional sources of recent information on utilizing NAA in selected fields, such as air pollution and



environmental analysis, food, forensic science, geological and inorganic materials as well as water analysis. NAA has been applied for determining many elements, usually trace elements, in the following fields and sample types:

1. Archaeology — amber, bone, ceramics, coins, glasses, jewellery, metal artefacts and sculptures, mortars, paintings, pigments, pottery, raw materials, soils and clays, stone artefacts and sculptures.
2. Biomedicine, animal and human tissues activable tracers, bile, blood and blood components, bone, brain cell components and other tissues, breast tissue, cancerous tissues, colon, dialysis fluids, drugs and medicines, eye, faeces, foetus, gallstones, hair, implant corrosion, kidney and kidney stones, liver, lung, medical plants and herbs, milk, mineral availability, muscle, nails, placenta, snake venom, rat tissues (normal and diseased), teeth, dental enamel and dental fillings, thyroid, urine and urinary stones.
3. Environmental science and related fields — aerosols, atmospheric particulates (size fractionated), dust, fossil fuels and their ashes, flue gas, animals, birds, insects, fish, aquatic and marine biota, seaweed, algae, lichens, mosses, plants, trees (leaves, needles, tree bark), household and municipal waste, rain and horizontal precipitations (fog, icing, hoarfrost), soils, sediments and their leachates, sewage sludges, tobacco and tobacco smoke, surface and ground waters, volcanic gases.
4. Forensics — bomb debris, bullet lead, explosives detection, glass fragments, paint, hair, gunshot residue swabs, shotgun pellets.
5. Geology and geochemistry — asbestos, bore hole samples, bulk coals and coal products, coal and oil shale components, crude oils, kerosene, petroleum, cosmochemical samples, cosmic dust, lunar samples, coral, diamonds, exploration and geochemistry, meteorites, ocean nodules, rocks, sediments, soils, glacial till, ores and separated minerals.
6. Industrial products — alloys, catalysts, ceramics and refractory materials, coatings, electronic materials, fertilizers, fissile material detection and other safeguard materials, graphite, high purity and high-tech materials, integrated circuit packing materials, online, flow analysis, oil products and solvents, pharmaceutical products, plastics, process control applications, semiconductors, pure silicon and silicon processing, silicon dioxide, NAA irradiation vials, textile dyes, thin metal layers on various substrates.



7. Nutrition — composite diets, foods, food colors, grains, honey, seeds, spices, vegetables, milk and milk formulae, yeast.
8. Quality assurance of analysis and reference materials — certification of element contents and homogeneity testing of mainly biological and environmental reference materials of chemical composition, method intercomparisons [5].

2.3.2 Neutron source

Three main sources of neutrons are available:

1. Research nuclear reactors (nuclear reactors used as neutron sources),
2. Ion and electron accelerators including neutron generators,
3. Radioactive sources.

In the present study a research nuclear reactor was used as neutron source. Research nuclear reactors have the highest neutron fluxes but are limited concerning their price and availability [3]. Research nuclear reactors are usually large devices in which fissionable material, almost exclusively ^{235}U , is fissioned into two nuclides with simultaneous emission of neutrons which induce further fissions in a chain reaction. The fission-produced are very energetic. The cross-section for neutron-induced fission of fissionable nuclides increases with decreasing energy of the neutrons, and in order to increase the neutron activity, moderators which slow the neutrons are added to the reactor. To reflect back some of the neutrons which leak from the reactor core, reflectors are used. The fission process releases large amounts of energy, mainly due to the stopping of the two recoiling fissioned particles, and the system is cooled by a coolant (either liquid or gas). Nuclear reactors are categorized according to their fuel, moderator, coolant reflector and configuration [3].

2.3.2.1 Sample introduction

The way of introducing a sample to the neutron flux depends on the physical structure of the reactor. It is essential that the introduction of the sample will not affect the operation of the reactor. The irradiation site may be within the reactor core or outside in the moderator/reflector region [3]. The samples are closed in sealed ampules in order not to be in contact with the water surrounding the core. For short irradiations a polyethylene capsule can be used. In order to have quick and reproducible sample introduction, mechanical systems are used. In the present study pneumatic devices were used. It is the most common system, owing to the shorter loading and unloading time and less



maintenance and failures than other systems such as chain-driven racks. In the pneumatic device, the sample is pushed along a tube with pressurized gas (air or nitrogen). The transfer time depends on the pressure and the distance transferred.

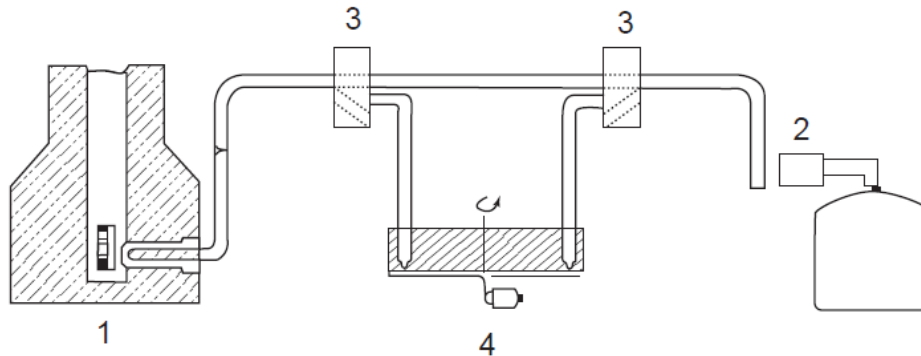


Figure 3: Schematic layout of a fast transfer pneumatic system for INAA, (1) Reactor; (2) Gamma-spectrometer; (3) Valves; (4) Sample changer; from [3]

2.4 GAMMA RAY SPECTROMETER

A typical analog gamma spectroscopy system consists of:

1. HPGe detector
2. High voltage power supply
3. Amplifier
4. Analogue to Digital Converter (ADC)
5. Multi-Channel Analyzer (MCA)

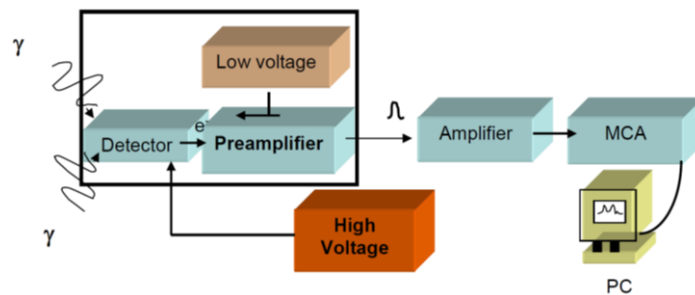


Figure 4: Block diagram of a basic gamma spectrometry system; from [7]

The function of this electronic system is the collection of the electrons produced from the signal pulses and the processing of those pulses and sorting them by height or energy.

This process can be described by the following steps:

1. Photon interacts with the detector crystal, produces burst of electrons
2. Applied bias voltage sweeps electrons from crystal
3. Current produced by electrons forms signal pulse
4. Pulse size is increased with a preamplifier



5. Pulse is further intensified and shaped with amplifier
6. Pulse intensity is converted into numerical value using ADC
7. Numerical values are sent to Multi-channel Analyzer (MCA)

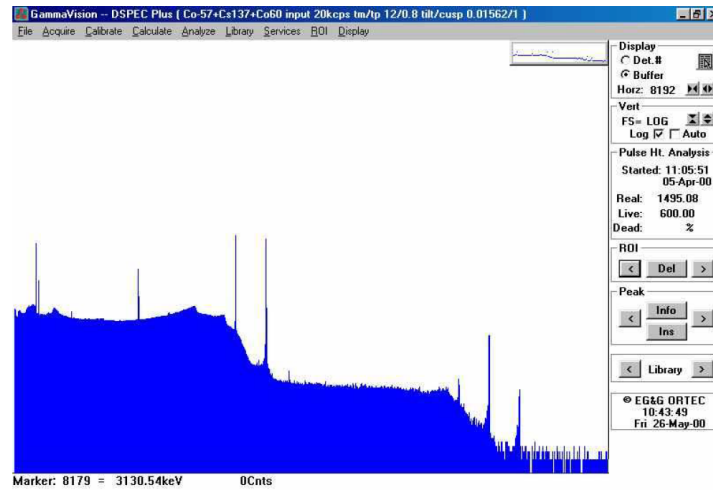


Figure 5: Typical Gamma ray Spectrum output visualized on a computer; from [7]

A computer is required in order to visualize the spectrum and perform basic spectrum analysis using spectrum analysis software [7].

2.4.1 HPGe detector

The detector is in fact the center piece of the gamma spectroscopy system. The gamma photons interact with the detection material and transfer their energies to electrons or to positrons in the case of annihilation. These produced particles lose their energy within the detector, creating ionized atoms and ion pairs. These secondary entities form the basis of the detector signal. High purity Germanium is the mostly used material for gamma ray spectrometry systems [7]. The detector used in the present study is a Germanium detector.

Germanium detectors are semiconductor diodes having a P-I-N structure in which the Intrinsic (I) region is sensitive to ionizing radiation, particularly X-rays and gamma rays. An electric field extends across the intrinsic or depleted region. When photons interact with the material within the depleted volume of a detector, charge carriers (holes and electrons) are produced and are swept by the electric field to the P and N electrodes. This charge, which



Figure 6: Different types of detectors; from [5]



is in proportion to the energy deposited in the detector by the incoming photon, is converted into a voltage pulse by an integral charge sensitive preamplifier [7].

2.4.1.1 Detector efficiency

Generally, the sensitivity of a HPGe system will be in direct proportion to the detector efficiency. The *efficiency of a detector* is a measure of how many pulses occur for a given number of gamma rays, i.e., the fraction of all the photons that are emitted by the source or sample (A), which cause an event in the detector (N). This is the efficiency ε of that detector.

$$\text{Equation 7} \\ N = \varepsilon \cdot A$$

Various kinds of efficiency definitions are in common use for gamma ray detectors. There is a lot of confusion surrounding this concept because users are often careless about what is meant by "an event in the detector". For some it means "a full energy event", and for others it means "any event that can be measured".

- *Absolute Efficiency*: The ratio of the number of counts produced by the detector to the number of gamma rays emitted by the source (in all directions).
- *Intrinsic Efficiency*: The ratio of the number of pulses produced by the detector to the number of gamma rays striking the detector. The intrinsic efficiency of a detector is defined in terms of the number of photons in a collimated beam incident on its entrance window; and not by the number of photons emitted by the source. This definition has the advantage that it is not tied to any source-detector geometry. It is often used to compare different detectors; but is of little importance when measuring the activity of radioactive samples.
- *Relative Efficiency*: HPGe detectors are almost universally specified in terms of their relative full-energy peak efficiency compared to that of a 3 in. x 3 in. NaI (Tl) Scintillation detector at a detector to source distance of 25 cm at 1.33 MeV.
- *Full-Energy Peak (or Photopeak) Efficiency*: The efficiency for producing full energy peak pulses only, rather than a pulse Efficiency curve of any size for the gamma ray. It is clear from the previous discussion that the photopeak efficiency of a detector will be dependent on the energy of the photon interacting with it.

Clearly, to be useful, the detector must be capable of absorbing a large fraction of the gamma ray energy. This is accomplished by using a detector of suitable size, or by choosing a detector material of suitable high Z. Detectors of greater than 100% relative



efficiency have been fabricated from germanium crystals ranging up to about 75 mm in diameter. About two kg of germanium is required for such a detector.

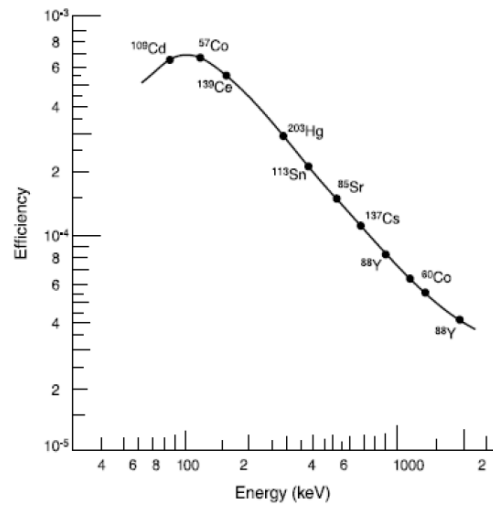


Figure 7: Example of a full-energy peak efficiency curve for germanium detector; from [7].

The counting efficiency of HPGe detectors is controlled by three major considerations:

Detector size

The larger the volume of the crystal, the larger the possibility that a photon will transfer all its energy to the Ge, and the higher the overall efficiency in general. The prices of these detectors also rise dramatically with increase in their volumes.



Figure 8: Two HPGe coaxial detectors of different sizes. The one to the left has a relative efficiency of 80%, the one to the right only 35%; from [7]

Photon energy

The efficiency value decreases for high energy photons (typically above 300 keV); approximately as $\varepsilon \propto E_{\gamma}^{-0.5}$. At lower values for the photon energy the photoelectric effect becomes very strong, and every photon falling in on the detector face is completely absorbed. When this state of 100 % absorption of photons is reached (typically below



about 100 keV), the intrinsic efficiency of the detector stays constant for the soft γ -photons.

Casing material

The detector is kept inside a small vacuum container to keep it at a low temperature. The canning is normally made from stainless steel to obtain a rigid container. This material will absorb some of the photons falling in on the entrance window before they can reach the Ge-material. This absorption in the window increases rapidly for energies below 100 keV. A combination of the last two effects results in a drop in overall efficiency at lower energies, and Ge-detectors can normally not be used below 80 keV.

The low energy range of the Ge-detector can be extended to about 50 keV by using aluminum as canning material, or even to about 30 keV using a beryllium entrance window. The semi-conducting material used for these low-energy detectors is usually flatter (i.e. a pancake form) than those used in high-energy work (similar dimensions for thickness and diameter). It is therefore important to place the sample to be counted in front of the entrance window.

One can obtain special detectors with a hole drilled into the detector material (and the canning too). These "well type" detectors have the advantage that a small sample can be placed inside the well, thereby maximizing the absolute efficiency of the detector. The diameter of the hole is normally less than 20 mm, and the detector can only be used for small samples. If enough sample material is available, a large sample outside the detector would probably give a higher count rate than a very small amount inside the well [7].

2.4.1.2 Detector resolution

Resolution is a measure of the width (full width half max, FWHM) of a single energy peak at a specific energy, either expressed in absolute keV (as with Germanium Detectors), or as a percentage of the energy at that point (Sodium Iodide Detectors). Better (lower FWHM value) resolution enables the system to more clearly separate the peaks within a spectrum. Figure 12 shows two spectra collected from the same source, one using a sodium iodide (NaI(Tl)) detector and one using germanium (HPGe). Even though this is a rather simple spectrum, the peaks presented by the sodium iodide detector are overlapping to some degree, while those from the germanium detector are clearly separated. In a complex spectrum, with peaks numbering in the hundreds, the use of a germanium detector becomes mandatory for analysis [7].



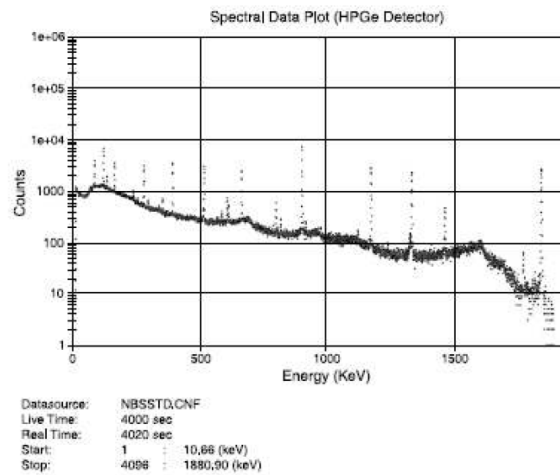


Figure 9: spectra collected using germanium (HPGe); from [7].

2.4.2 High voltage power supply

The High Voltage Power Supply unit supplies the necessary high voltage to the detector and the necessary voltages to the rest of the system components. These units are usually able to supply up to 5000 V. Typical HPGe detectors require about 3000 V [7].



Figure 10: Typical HV power supply; from [5]

2.4.3 Amplifier



The amplifier serves to shape the pulse as well as further amplify it. In this module the size (height) of the pulses are increased, and their form carefully manipulated to eliminate problems with electronic noise, shifts in the baseline, and pulses "riding" on the tails of those preceding them [7].

Figure 11: Typical amplifier; from [5]

2.4.4 Analogue to Digital Converter (ADC)

The analog-to-digital conversion module (ADC) forms the heart of the gamma spectrometer. It converts the analog information from the pulse train into a digital format that can be stored and processed by a computer. For each analog pulse received by the ADC, a number is generated that is proportional to the height of that pulse [7].

ADC requires some time to process an incoming pulse. During this period, known as the *dead time* of the instrument, it cannot accept another pulse. This second pulse is therefore



lost [6]. Thus, low dead times are required so less information gets lost, below 10% would be desirable.

2.4.5 Multi-Channel Analyzer (MCA)

The multichannel analyzer (MCA) is the heart of most experimental measurements. It performs the essential functions of collecting the data, providing a visual monitor, and producing output, either in the form of final results or data for later analysis.

The multichannel analyzer (MCA) consists basically of an analog-to-digital converter (ADC), control logic, memory and display. The multichannel analyzer collects pulses in all voltage ranges at once and displays this information in real time [7].

2.5 SPECTRUM FORMATION

The characteristic gamma rays of a given radionuclide that is present in the analyzed sample are emitted with one or more well-known energies. These gamma rays are detected by the detector, treated by the electronic setup and then observed in the form of a spectrum. In this chapter, we will describe the different processes that are involved in the spectrum formation and study the different spectrum components.

2.5.1 Origin of X and γ radiation

After a nucleus has emitted a beta particle, often it is still slightly unstable and will get rid of its excess energy by emitting a gamma ray immediately afterwards. The time delay between the two emissions is so short (less than a billionth of a second) that we look upon them as being simultaneous, and as being only one disintegration.

Light, radio waves, X-rays and gamma rays are all "electromagnetic" radiation. They differ from one another only in their frequencies.

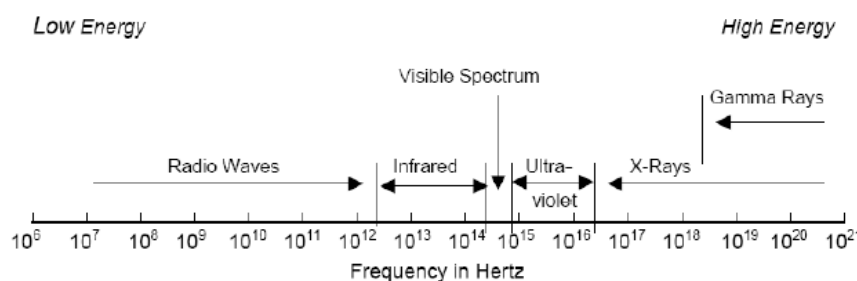


Figure 12: Electromagnetic spectrum; from [7].

The energy of any electromagnetic radiation depends on its frequency. In fact, the energy and frequency are directly proportional. X and gamma rays have the highest energies.



They cover about the same range of frequencies and, in fact, the only difference between them is their origin. Gamma rays are emitted from the nuclei of radioactive atoms, while X-rays are produced by disturbances in the electron orbits of atoms. X-rays are not emitted from nuclei.

2.5.2 Photon interaction with matter

The most important interaction of α , β and γ -rays is by ionization, where some electrons are ejected from neutral atoms leaving positively charged ions behind. This process can be readily visualized for the α - and β -particles which are both electrically charged, but it is more difficult for γ -rays which are electrically neutral electromagnetic waves. It is, however, essential that the interaction is understood in order to apply the knowledge to γ -spectrometry. Gamma photons produce ionization indirectly as a result of collisions. There are three ways in which a gamma photon can interact with an atom:

- The photo-electric effect
- The Compton scattering
- The pair production

Photo-electric effect

In the photoelectric process, all the energy of the incident photon ($h\nu$) is transferred to a bound electron near the nucleus of the atom. This electron is then ejected from that atom with a kinetic energy of:

$$\begin{array}{c} \text{Equation 8} \\ E = h\nu - I \end{array}$$

where I denotes the energy required to remove a bound electron from that atom. In this effect it is the *binding energy* for the K- and L-shell electrons to that atom.

The high energy electron is in all respects the same as a β -particle and can cause secondary ionization in the medium. It is assumed that this electron will lose all its energy in the material. It is important to note that the photon "disappears" in this process.

The following aspects concerning the electrons are important for understanding this effect:

- The photoelectric effect involves mainly those electrons that are closely bound to the nucleus (i.e. the inner orbitals) in the K- and L-shells. The probability for the effect becomes less for the electrons that are more loosely bound in outer orbitals.



- If the energy of the incident photon is less than the ionization potential or binding energy of an electron in a particular inner shell (i.e. if $h\nu < I_K$), that electron cannot be involved in the photoelectric effect. Less tightly bound electrons in other (outer) orbitals are, however, then available if $h\nu > I_L$.

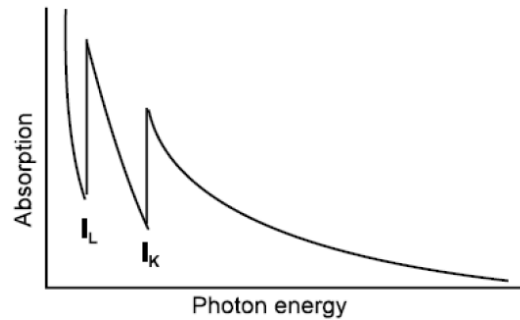


Figure 13: Probability of the photoelectric effect; from [7]

The probability for the photoelectric effect is also determined by a number of other aspects:

- The higher the energy of the incident photon (above the $h\nu > I_{\text{limit}}$), the smaller the chance for the effect to occur.
- The higher the atomic number of the absorbing material, the bigger the chance for the effect.

Compton effect

If the gamma photon energy is not low enough for this, Compton scattering is more likely. Here, the photon will transfer only part of its energy to an electron. The remaining energy is taken away by a new gamma photon of lower energy. We say that this new photon is *scattered*, because it will take off in a new direction. The electron that was ejected from the atom produces ionizations in just the same way as a beta particle.

This process differs from the photoelectric effect in that:

- I. The photon transfers only a fraction of its energy to the electron, and
- II. Only the (essentially) free electrons in the outer orbitals are involved in the process.

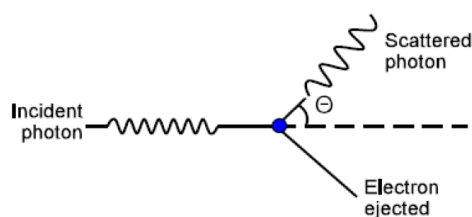


Figure 14: Compton effect; from [7].



The photon is reflected (or scattered) through an angle (Θ) with the respect to the line of incidence (see Figure 14) and moves along with decreased energy.

The maximum energy that a photon can transfer to an electron is when $\theta = 180^\circ$, i.e. when the photon is scattered directly backwards (and the electron moves in the direction of the incident photon). This is still less than the total energy that can be transferred by the same photon in a *photoelectric interaction*. The scattering angle can be any value between 0 and 180. And the smaller the angle, the smaller the amount of energy that is transferred to the electron. A photon just "grazing" an electron ($\theta = 0^\circ$) transfers no energy.

The probability for Compton interaction increases with the atomic number of the absorber and decreases with the energy of the incident photon. An interesting situation develops for the geometric arrangements normally used for counting samples: the sample is placed close to the detector inside a heavy shield (normally lead). The detector therefore "sees":

- a. Photons directly from the sample, and
- b. A smaller number that were all reflected by approximately 180° from the absorber.

This backscattering produces photons with more or less the same energy, regardless of the energy of photons incident on the lead shield. The *backscattered photons* appear as a broad peak in the low-energy region of the pulse height spectrum.

Pair production

A high-energy gamma photon sometimes changes into two electrons, one positive and the other negative. The positive electron is called the *positron*. This interaction is known as pair production, for obvious reasons. This effect can be explained in terms of the relativity theory which postulates that "matter" and "energy" are different forms of the same entity. A particle of mass m can be converted into an amount of energy E , and viceversa, according to the famous equation $E = mc^2$, where c is the speed of light.

Pair production is one consequence of this theory. A photon with energy E is converted into two different particles with the same mass, but with opposing electrical charges. The excess energy (i.e. more than the minimum required to produce the particles) is shared by the two particles in the form of kinetic energy

The two particles involved are both electrons. One, the electron, is negatively charged, the other, is the positive electron, or *positron*. It has the same mass and nuclear properties



as the negative electron, but with the opposite electrical charge. The term *negatron* is sometimes used to distinguish the negative from the positive electron.

The positron at rest is not a stable particle. Once it has been produced by pair production, the positron will lose energy by interaction with electrons in the absorbing material in the same manner that a negatron does. But when it has lost all its kinetic energy, it cannot exist in the presence of other electrons, and a nuclear reaction occurs. In this reaction a positron and negatron pair destroys (*annihilates*) each other with the production of two photons with energy of 511 keV each. This annihilation can occur between the positron and any electron; not necessarily with the one formed during the pair production.

Pair production is only possible if the energy of the incident photon is sufficient to provide at least the mass of a positron and negatron pair (> 1022 keV). In practice it is only significant for photon energies above 1.5 MeV. The higher the photon energy, the more likely pair production is to occur.

Combined effect

The three effects through which γ -rays can interact directly with, and transfer energy to matter, were discussed separately in the preceding sections. It is, however, also possible that two or more different events can occur in sequence for the same primary photon. A Compton scattered photon can be totally absorbed by a photoelectric event, or it can be scattered again by a second Compton interaction. Similarly, one or both of the photons that result from the annihilation of the negatron produced in pair production, can be scattered once or repeatedly. Two situations should be distinguished when considering the overall effect of the interaction of gamma rays with matter:

- One can consider a collimated beam of photons and focus on what happens to this beam when it traverses a layer of absorbing material. This is normally the approach when one studies shielding and safety.
- One can also focus on the absorbing material and try to determine how much energy was transferred to it. Since the purpose of γ -spectrometry is to determine the energy of individual photons, and the "material" is normally the detector, this is the major concern.



2.5.3 Pulse height spectrum

For gamma ray spectrometry, only the *height of the pulses* is important; and not the time when the events occurred. The objective is therefore to convert the train of pulses produced by the detector, into information that can be used by the analyst to determine the energy and intensity of the photons emitted by the source.



Figure 15: Train of pulses delivered at the output detector; from [7]

The pulses delivered at the output of the detector are "sorted" or classified according their height as shown in Figure 15. The number of pulses in each category are then counted; with each counter representing a pulse height interval. There are two concepts involved in this process:

- The index number or code of each counter. (These codes normally run from "1" to higher values as required. They are referred to as channels in gamma spectrometry.)
- The number of pulses collected in each counter (i.e. the contents of that counter).

If the contents of each channel are plotted (on the vertical axis) against the number of that channel (on horizontal axis), one obtains a pulse height spectrum as shown in Figure 16.

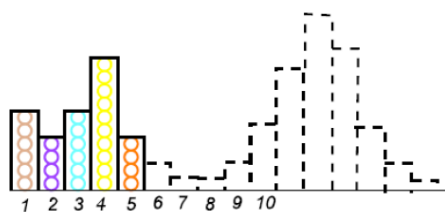


Figure 16: Pulse height spectrum; from [7]

The second illustration is derived from the first one. It is, however, impossible to reconstruct the original train of pulses from this figure because both their actual sizes and the time when they occurred, have been lost in the processing of the data.



2.5.4 Energy transferred to the detector

The prime concern for γ -spectrometry is the energy of the photon that must be measured. It is clear that the amount of energy deposited in the absorber material (i.e. the detector) will be equal to the photon energy in the following cases only:

- A photoelectric event,
- One or more Compton scatterings followed by a photoelectric event,
- Pair production followed by photoelectric absorption of both annihilation photons; which might have been preceded by one or more Compton scatterings.

In each of these cases the sequence stops in a photoelectric event. It is, however, more correct to refer to these as full energy events, and not as "photoelectric" events.

An interesting situation can develop when a high energy photon ($E > 1022 \text{ keV}$) starts the sequence: Some of the annihilation photons can escape from the detector. No distinction can be made between the two photons produced on annihilation of the positron, and the following cases can be distinguished:

- Both annihilation photons are totally absorbed: total energy event,
- Only one annihilation photon is totally absorbed, while the other escapes from the detector: single escape event,
- None of the two photons are totally absorbed: double escape event.

2.5.5 Spectrum components

The spectrum is composed by different kind of peaks:

- i. Full energy peak (FEP)
- ii. Compton continuum and Compton edge
- iii. Sum peak
- iv. Other components of the spectrum such as single escape peaks, double escape peaks or annihilation peaks.



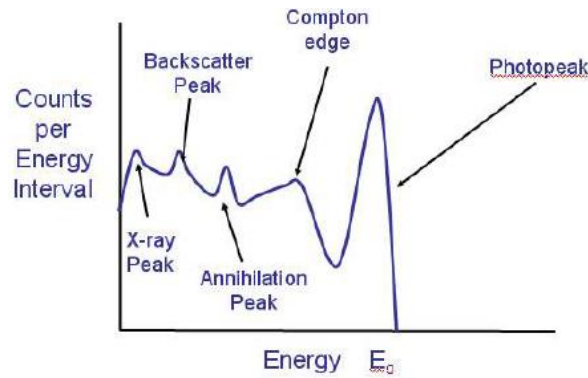


Figure 17: Components of Spectrum; from [7].

Full energy peak (FEP)

A full energy peak is the result of detecting full energy events.

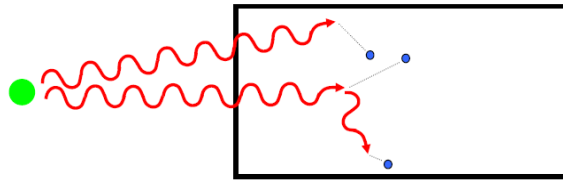


Figure 18: Full energy event; from [7].

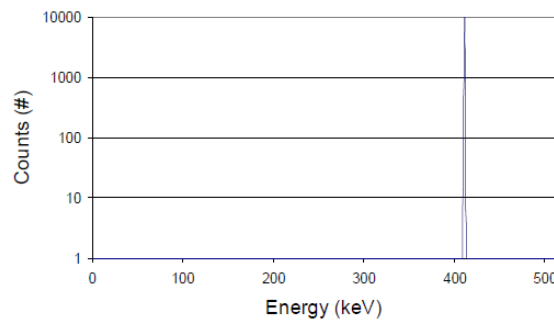


Figure 19: Full energy peak (FEP); from [7].

Compton continuum and Compton edge

The scattered gamma-ray will inevitably escape from the detector, taking with it the remaining gamma-ray energy. The detector response to Compton interactions will, therefore, mirror the curve shown in Figure 21 and the corresponding gamma-ray spectrum would exhibit the characteristic *Compton continuum* extending from zero energy up to the *Compton edge* illustrated on the right hand side of Figure 21. There would be no Compton scattering contribution to the full energy peak.



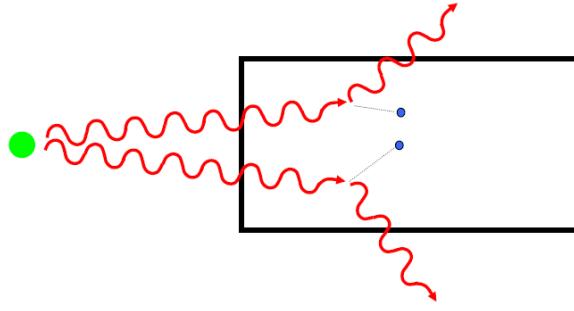


Figure 20: Scattered gamma-rays escape from the detector; from [7].

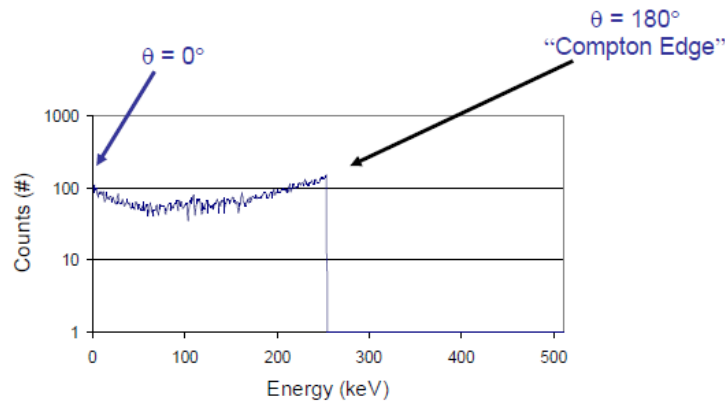


Figure 21: Compton edge and continuum; from [7].

Sum peak

When an isotope emits more than one cascade gamma rays in its decay process, there is a chance that both will deposit energy in the detector [7]. If we assume that no isomeric states are involved the lifetime of the intermediate state is generally so short that the two gamma rays are, in effect, emitted in coincidence. It is then quite possible for both gamma-ray photons from a single decay to interact and deposit all their energy within a time that is short compared with the response time of the detector or the resolving time of the following electronics [8]. When this happens, a *sum peak* can be observed in the spectrum. Sum peaks can also be observed in samples containing isotopes that emit only one photon per decay. This is generally only true for high activity samples [7].

2.5.6 Background

Because of the cosmic radiation that continuously bombards the Earth's atmosphere and the existence of natural radioactivity in the environment, all radiation detectors record some *background signal*. The nature of this background varies greatly with the size and type of detector and with the extent of shielding that may be placed around it. The background counting rate can be as high as many thousands of counts per second for large-volume scintillators, to a few counts per day in some specialized application. Because the magnitude of the background ultimately determines the minimum detectable



radiation level it is most significant in those applications involving radiation sources of low activity. However, background is often important enough in routine usage so that the majority of radiation detectors are provided with some degree of external shielding to effect a reduction in the measured level. A second purpose of detector shielding is to provide a degree of isolation in laboratories where other radiation sources may be used or moved about during the course of a measurement.

The greatest value of keeping background small is encountered when extremely weak sources of radiation must be detected. The term *low-level counting* is often applied to such applications.

The sources of background radiations can be conveniently grouped into five categories:

1. The natural radioactivity of the constituent materials of the detector itself,
2. The natural radioactivity of the ancillary equipment, supports, and shielding placed in the immediate vicinity of the detector,
3. Radiations from the activity of the Earth's surface (*terrestrial radiation*), construction materials of the laboratory, or other far-away structures.
4. Radioactivity in the air surrounding the detector,
5. The primary and secondary components of cosmic radiation

The importance of various components of the background changes greatly with the circumstance. In gamma-ray detectors without shielding, the terrestrial and cosmic ray components are normally dominant. When significant shielding is provided, both the cosmic flux and the background caused by ambient sources of gamma rays are decreased, and radioactive contamination of structural and shielding materials around the detector becomes an important fraction of the remainder.

Using shielding of the type shown in Figure 22, a typical detector background is made up of a 30% contribution from cosmic radiation, 60% from the radioactive contamination of shielding materials and 10% from radioactivity within the detector and unidentified sources.



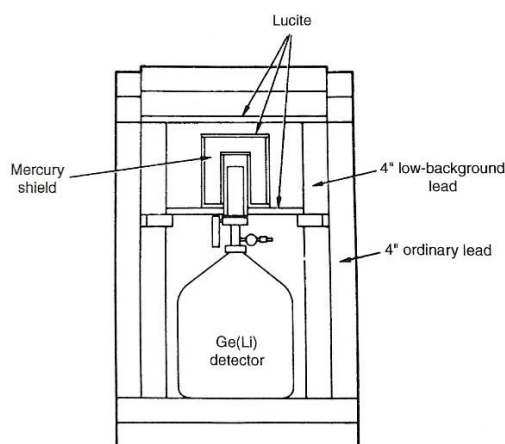


Figure 22: A low-background shield configuration for a germanium detector; from [8].

Typical background spectra from this configuration is shown in Figure 23 [8].

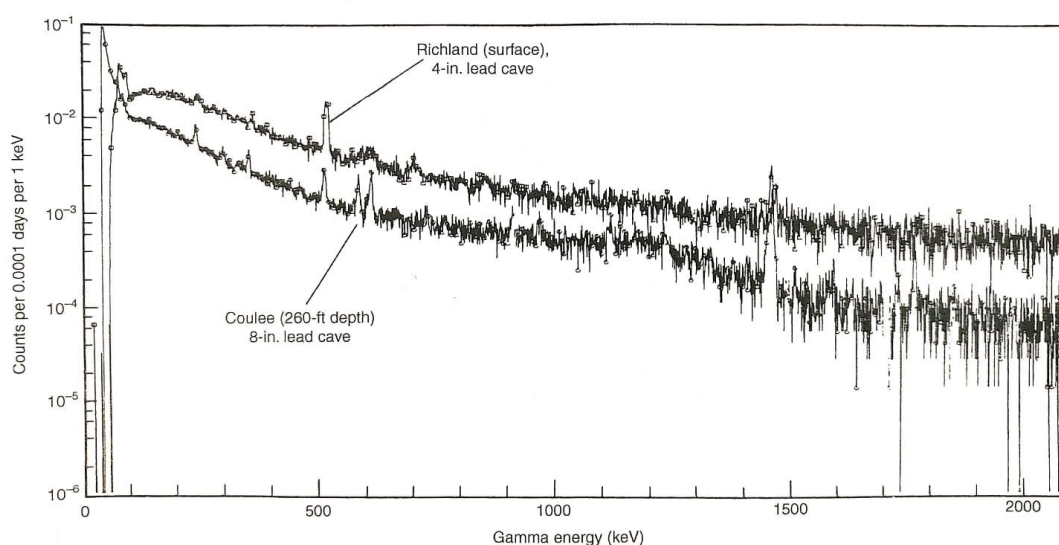


Figure 23: Background spectrum recorded for a Ge detector using the shielding shown on Figure 22; from [8].

In gamma-ray spectroscopy, some additional interfering radiation can be observed as a result of the interaction of primary gamma rays from the source with structural and shielding materials around the detector. The origins of these source-related background events can be Compton backscattering of the primary gamma rays, and the generation of secondary annihilation photons and characteristic X-rays through pair production or photoelectric absorption. These effects can be eliminated only by removing all materials from the immediate vicinity of the detector, but the practical demands of shielding usually do not permit this approach. Therefore, the potential source regions for these secondary radiations, particularly the inner surface of the radiation shield, are often designed with materials intended to reduce their importance [8].



3 METHODOLOGY

3.1 PREPARATION OF THE SAMPLE

INAA is one of the simplest techniques for trace element analysis. First step is to cut a small sample of the depleted uranium, as it can be observed in Figure 24.



Figure 24: Sample of depleted uranium being cut at the left and final shape of the sample at the right.

In order to measure the weight of the depleted uranium sample first the plastic bag that was going to contain it was weighed alone, then the plastic bag with the sample inside was weighed and thus by a simple subtraction the weight of the uranium is determined.



Figure 25: Weighing procedure.

Equation 9

$$m_{\text{sample}} = 0.4024 - 0.2543 = \mathbf{0.1481 \text{ grams}}$$

Samples are inserted into polyethylene or polypropylene cans for short irradiation or into a quartz vial which is inserted in an aluminum can for long irradiation. The length of the



irradiation for the current study is short – only 15 minutes –, thus the capsule was made of polyethylene (see capsule in Figure 26). PVC cans or glass vials cannot be used, since they will become very radioactive owing to the formation of ^{38}Cl or ^{24}Na , respectively.

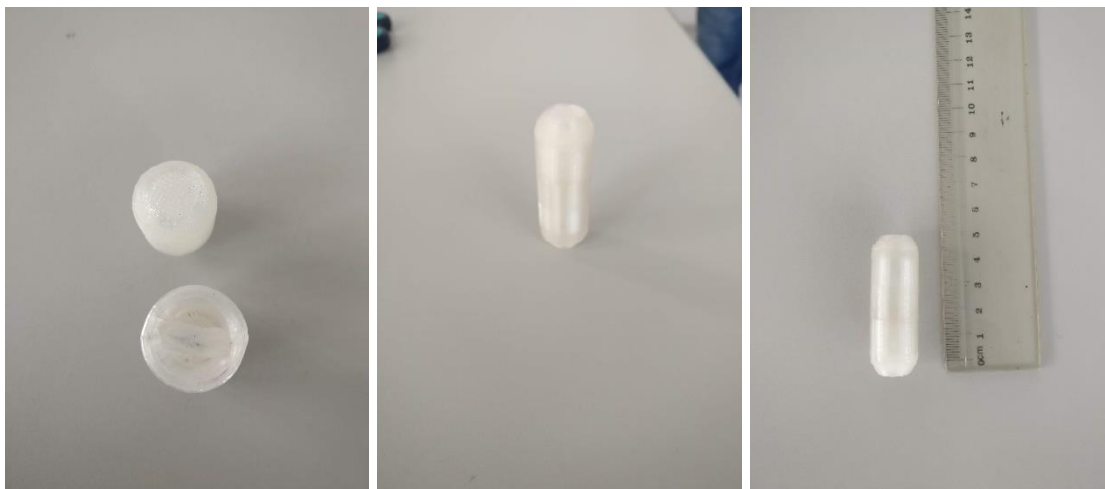


Figure 26: Sample in the plastic capsule.

For a short irradiation time the sample is ‘sent’ alone to the reactor by means of a pneumatically operated tube (see Figure 27).



Figure 27: Pneumatic system. Terminal at the laboratory at the left side and terminal at the reactor to the right.

3.2 IRRADIATION

Once the sample is inside the reactor, the *irradiation time* starts. 15 minutes of irradiation is the optimal time so that the dead time is not too high when measuring short life products. The operating conditions of the reactor during the irradiation were the following:





Figure 28: Operating conditions of the reactor.

3.3 MEASUREMENTS

After the sample has been removed from the reactor, they are counted (this means taking a γ -ray spectrum) immediately or the γ -ray spectrum is taken after some ‘cooling’ (decay) time, to reduce the high radioactivity level due to short-lived radionuclides.

Four different measurements were performed using this same depleted uranium sample. Find all the details in the following table:

Measurement 1	
Acquisition time	10:38:09 (12/04/2019)
Cooling time	129 s
Live time	418.7 s
Real time	429.6 s
Dead time	2.53%
Distance	120 mm
Measurement 2	
Acquisition time	10:47:17 (12/04/2019)
Cooling time	677 s
Live time	909 s
Real time	945.4 s
Dead time	3.86 %
Distance	80 mm
Measurement 3	
Acquisition time	11:04:29 (12/04/2019)
Cooling time	1709 s
Live time	6294.9 s
Real time	6492.8 s



Dead time	3.05 %
Distance	30 mm
Measurement 4	
Acquisition time	14:48:12 (10/05/2019)
Cooling time	2434332 s ¹
Live time	249064.4 s
Real time	249498.7 s
Dead time	0.17 %
Distance	3 mm

The γ -spectra of each one of the measurements is obtained using the software *Genie 2000* with an MCA with 0-16000 channels.

¹ 28,17513889 days.



4 RESULTS

The result of the measurements by the analyst is:

- (i) a set of typically 8192 numbers that represent the pulse height spectrum; and
- (ii) a few numbers that describe the energy and efficiency calibration of the detector.

This section describes how these data are processed to provide information on the identity and activity of all the nuclides that are present in the sample that was counted.

The *nuclide library* is essential in this process. It is a list (inventory) of nuclides which are selected by the analyst in advance, and which contains at least the following information:

- For every nuclide listed: The isotope symbol (e.g. ^{60}Co) and the half-life.
- For every photon-line emitted by this nuclide: The accepted photon energy (keV) and the yield of that line (number of photons per disintegration).

In this case, all the nuclides with *yield* value bigger than 0.03 from *Janis database* (see reference [9]) were selected. With this set of nuclides *Decay search* (see reference [10]) was then used to create the nuclide library previously explained. So, the final nuclides present in the nuclide library have the following characteristics:

- Yield bigger than 0.03.
- Only peaks with *intensity* (I_γ) bigger than 20 %.
- From the results, only peaks with *area* bigger than 1000 and *error* (%err) lower than 10%.
- No meta-stable nuclides.

After that, using the nuclide library all the fission products from each measurement are identified considering the cooling time of each measurement and the half-life of each nuclide. It wouldn't make sense to look for nuclides with very short half-life in measurements with very long cooling time.

Once all the fission products are identified, for each single one of the peaks that indicate its presence the following values are calculated:



Self-shielding correction

Only for peaks of energy with *values of energy lower than 400 keV* the following correction for *self-shielding* was applied:

$$\text{Correction} = \frac{MAC \cdot \rho \cdot d}{1 - e^{-MAC \cdot \rho \cdot d}}$$

Where:

MAC: Total attenuation with coherent scattering in cm²/g.

ρ: Density of Uranium, 19.1 g/cm³.

d: thickness of the foil in cm.

Saturated activity (A_{SAT})

$$A_{SAT} = \frac{S(E_\gamma) \cdot \lambda \cdot \frac{t_{real}}{t_{live}}}{I_\gamma(E_\gamma) \cdot \varepsilon(E_\gamma) \cdot (1 - e^{-\lambda \cdot t_{irr}}) \cdot e^{-\lambda \cdot t_{cool}} \cdot (1 - e^{-\lambda \cdot t_{real}})}$$

Where:

$S(E_\gamma)$: Area of the peak.

λ: Decay constant (see Kinetics of Decay of Radioactive Nuclides in page 17 for how to calculate it using the half-life).

t_{real} : Real time in seconds.

t_{live} : Live time in seconds.

$I_\gamma(E_\gamma)$: Absolute value of the intensity of the peak.

$\varepsilon(E_\gamma)$: Absolute value of effectivity, which depends on the energy of the peak but also on the distance used for the measurement.

t_{irr} : Irradiation time in seconds.

t_{cool} : Cooling time in seconds.

Number of target nuclei (N_0)

$$N_0 = \frac{m \cdot N_A}{M_U} \cdot C$$

Where:

m: mass of the sample in grams (see Preparation of the sample in page 40 for this measurement).

N_A : Avogadro constant.



M_U : Mass number of the uranium in the sample, so 238.

C : concentration of the uranium.

Reaction rate (R_R)

$$R_R = \frac{A_{SAT}}{N_0}$$

Where:

A_{SAT} : Saturated activity.

N_0 : Number of target nuclei.

Reaction rate for fission (RR_f^i)

$$RR_f^i = \frac{R_R}{Y}$$

Where:

R_R : Reaction rate.

Y : Yield.

Deviation (σ_i)

$$\sigma_i = err \cdot R_R$$

Where:

err : Absolute value of the error (% err) given by the results of the γ -spectrometer.

R_R : Reaction rate.

After all this, the *Reaction Rate for fission of each one of the measurements “j”* from 1 to 4 can be calculated with the following formula:

$$RR_{f_j} = \frac{\sum_i \frac{RR_f^i}{\sigma_i^2}}{\sum_i \frac{1}{\sigma_i^2}}$$

Where:

RR_f^i : Reaction rate for fission of each peak.

σ_i : Deviation of each peak.



Then using the fact that $\sigma_j^2 = \frac{1}{\sum_i \frac{1}{\sigma_i^2}}$; the average *Reaction Rate for fission* is calculated using the following expression:

$$RR_f = \frac{\sum_j \frac{RR_{fj}}{\sigma_j^2}}{\sum_j \frac{1}{\sigma_j^2}}$$

Where:

RR_{fj} : Reaction Rate for fission of each one of the measurements “j” from 1 to 4.

σ_j : Deviation of each one of the measurements “j” from 1 to 4.



4.1 RESULTS OF THE FIRST MEASUREMENT

Irradiation time	900 s
Irradiation end	10:36:00 (12/04/2019)
Acquisition time	10:38:09 (12/04/2019)
Live time	418,7 s
Real time	429,6 s
Dead time	2,53 %
Distance	120 mm
Cooling time	129 s
Sample's weight	0,1481 g
Number of target nuclei	1,12422E+18
d	2,83E-02 cm
ρ	1,91E+01 g/cm ³

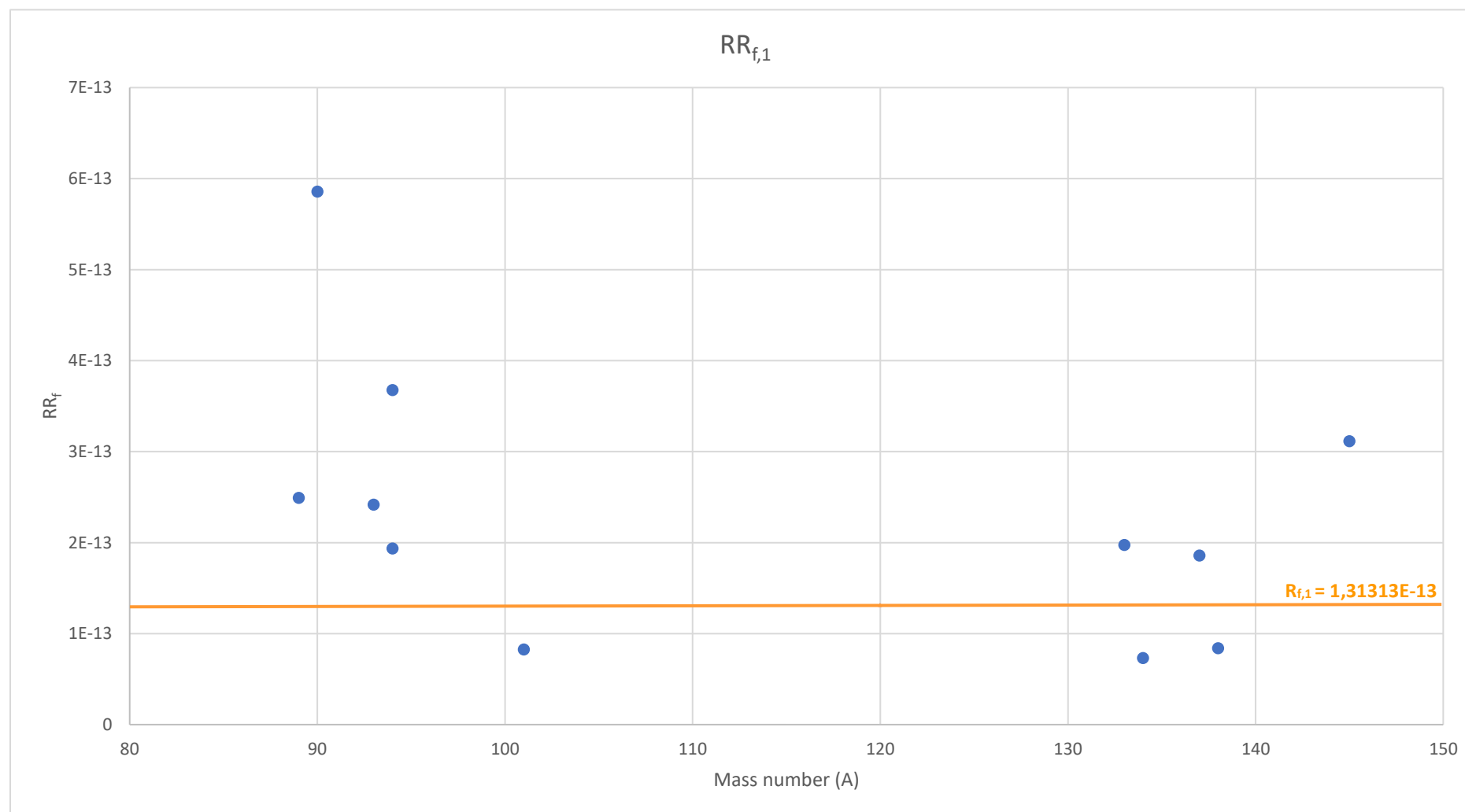
Effectivity for 120mm distance		
	koef	err
a=	-6,7462434	
b=	-0,9184971	
c=	-0,0230286	
d=	-0,0211147	
e=	0,03829395	
f=	0,02660976	
g=	0	
h=	0	

Self-shielding correction		
Product	Energy [MeV]	MAC [cm ² /g]
Tc101	0,30709	4,94E-01
Te133	0,31231	4,77E-01
Xe138	0,25874	7,17E-01

Product	Yield	T1/2 [s]	λ	Pk	Energy	Self-shielding correction factor	Area	%err	Intensity	Effectivity	Saturated activity	RR _f ⁱ	Deviation σ_i	Deviation σ_i [%]
Sr94	0,0606287	75,3	0,00920514	96	1427,91		319	8,7	94	0,000844699	12687,5049	3,67594E-13	3,19807E-14	8,70
Rb90	0,0449896	158	0,00438701	65	831,35		874	6,6	39,9	0,001391731	15000,01928	5,85666E-13	3,8654E-14	6,60
I134	0,0782964	3132	0,00022131	68	846,89		298	8,1	95,4	0,001368395	3256,27816	7,30551E-14	5,91746E-15	8,10
Tc101	0,0517255	853,2	0,00081241	20	307,09	1,14	1107	4,2	89	0,003532175	2133,21351	8,25334E-14	3,4664E-15	4,20
Sr93	0,0623749	445,38	0,00155631	47	590,32		2118	2,5	68	0,001904482	8688,153285	2,4176E-13	5,46622E-15	2,26
			0,00155631	69	875,78		549	8,8	24,5	0,001327101	8969,94583			
			0,00155631	71	888,05		427	6,6	22,1	0,001310332	7833,246633			
Te133	0,0305767	750	0,0009242	21	312,31	1,13	1131	4	62	0,003476238	3029,458381	1,974E-13	7,896E-15	4,00
Ce145	0,0393304	180,6	0,00383802	56	724,11		786	8,9	59	0,001578771	6969,958397	3,11295E-13	2,77053E-14	8,90
Rb89	0,0471522	909	0,00076254	83	1031,78		706	7,2	58	0,001141968	6633,849587	2,49104E-13	1,44548E-14	5,80
			0,00076254	89	1248,18		445	9,8	42,6	0,000957565	6789,299373			
Y94	0,064527	1122	0,00061778	74	918,63		732	8	56	0,001270379	7104,488772	1,93402E-13	1,54722E-14	8,00
Xe138	0,0629685	844,8	0,00082049	16	258,74	1,2059	573	7,5	31,5	0,004141628	2649,989673	8,38551E-14	2,66201E-14	31,75
			0,00082049	32	434,85		866	9,4	20,3	0,002535466	10151,61758			
Xe137	0,0612832	229,08	0,00302579	34	455,55		722	5,6	31	0,002426247	6478,274184	1,8569E-13	1,03986E-14	5,60

Reaction rate for fission of the first measurement: **RR_{f,1} = 1,31313E-13**; Deviation σ_i : **2,20203E-15**; Deviation σ_i [%]: **1,68%**.





4.2 RESULTS OF THE SECOND MEASUREMENT

Irradiation time	900	s
Irradiation end	10:36:00	(12/04/2019)
Acquisition time	10:47:17	(12/04/2019)
Live time	909	s
Real time	945,4	s
Dead time	3,86	%
Distance	80	mm
Cooling time	677	s
Sample's weight	0,1481	g
Number of target nuclei	1,12422E+18	
d	2,83E-02	cm
ρ	1,91E+01	g/cm ³

Effectivity for 80mm distance		
	koef	err
a=	-6,1206892	
b=	-0,9070547	
c=	-0,0317684	
d=	-0,0670639	
e=	0,01291568	
f=	0,02255786	
g=	0	
h=	0	

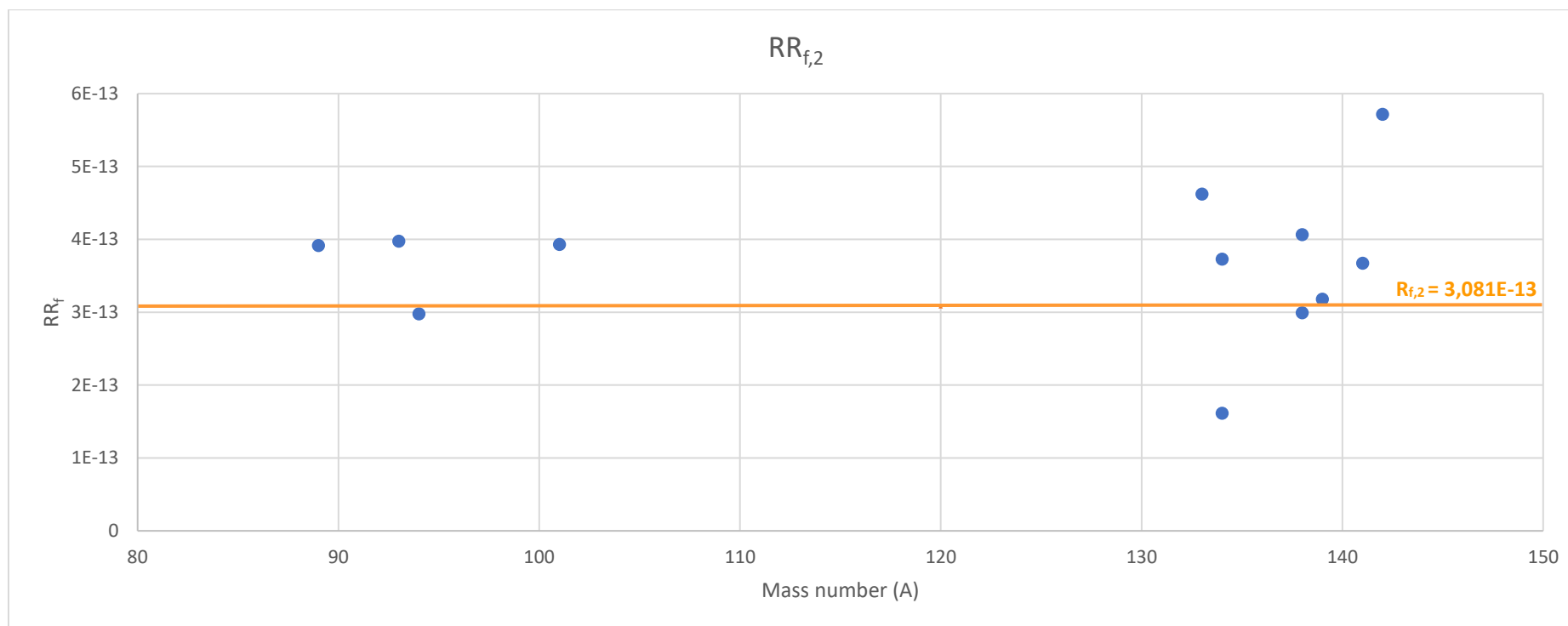
Self-shielding correction		
Product	Energy [MeV]	MAC [cm ² /g]
Tc101	0,30711	4,94E-01
Te133	0,31231	4,77E-01
	0,19068	1,454
Ba141	0,30447	5,03E-01
Xe138	0,25869	7,17E-01
Te134	0,2108	1,147
Ba139	0,16621	2,021

Product	Yield	T1/2 [s]	λ	Pk	Energy	Self-shielding correction	Area	%err	Intensity	Effectivity	Saturated activity	Reaction rate	Deviation σ_i	Dev. σ_i [%]
I134	0,0782964	3132	0,00022131	113	846,83		2063	2,6	95,4	0,002553094	6642,300308	1,61151E-13	3,13645E-15	1,95
			0,00022131	119	883,94		1669	2,9	64,9	0,002456188	8210,779658			
Tc101	0,0517255	853,2	0,00081241	44	307,11	1,14	11439	1,1	89	0,00666797	10152,73456	3,92796E-13	4,32076E-15	1,10
Cs138	0,0670757	2004,6	0,00034578	157	1436,05		2051	3,2	76,3	0,001571183	10426,85995	2,99235E-13	5,27511E-15	1,76
			0,00034578	68	462,8		2996	2,5	30,7	0,004464497	13322,01881			
			0,00034578	133	1009,5		1087	3,8	29,8	0,002178174	10206,10017			
Sr93	0,0623749	445,38	0,00155631	85	590,38		4336	2,8	68	0,003547154	14374,71143	3,97451E-13	9,26278E-15	2,33
			0,00155631	117	875,86		1031	4,2	24,5	0,002476624	13587,2409			
Te133	0,0305767	750	0,0009242	45	312,31	1,13	5410	1,7	62	0,00655923	7265,799283	4,6189E-13	7,33568E-15	1,59
			0,0009242	59	407,87		1766	4,4	27,1	0,005046064	7053,412425			
Rb89	0,0471522	909	0,00076254	136	1031,7		2634	3,1	58	0,002135553	11079,55423	3,91344E-13	1,04517E-14	2,67
			0,00076254	149	1248,1		1371	5,2	42,6	0,00179283	9352,629428			
Y94	0,064527	1122	0,00061778	124	918,56		2809	2,1	56	0,002372469	10939,19027	2,97793E-13	6,25365E-15	2,10
La142	0,0584862	5466	0,00012681	90	641,44		2491	5	47	0,003285618	19023,98035	5,71372E-13	2,85686E-14	5,00
Ba141	0,0582849	1096,2	0,00063232	26	190,68	1,44	7821	1,4	46	0,010212819	8602,445479	3,67166E-13	4,39272E-15	1,20
			0,00063232	43	304,47	1,14	3368	2,3	25,4	0,006724502	10189,22984			



Product	Yield	T1/2 [s]	λ	Pk	Energy	Self-shielding correction	Area	%err	Intensity	Effectivity	Saturated activity	Reaction rate	Deviation σ_i	Dev. σ_i [%]
Xe138	0,0629685	844,8	0,00082049	39	258,69	1,21	5373	1,7	31,5	0,007865146	11446,96647	4,06547E-13	6,2798E-15	1,55
			0,00082049	62	434,9		4270	3,4	20,3	0,004740696	23419,66147			
Te134	0,069725	2508	0,00027637	103	767,09	1,34	1602	6,1	29,5	0,002791624	13314,78477	3,72614E-13	1,2719E-14	3,41
			0,00027637	30	210,8		3669	4,1	22,7	0,009438853	11720,69297			
Ba139	0,064134	4983,6	0,00013909	21	166,21	1,64	1707	4,7	23,7	0,011180583	7062,593263	3,17711E-13	1,49324E-14	4,70

Reaction rate for fission of the second measurement: $RR_{f,2} = 3,081E-13$; Deviation σ_i : $1,70204E-15$; Deviation σ_i [%]: **0,55%**.



4.3 RESULTS OF THE THIRD MEASUREMENT

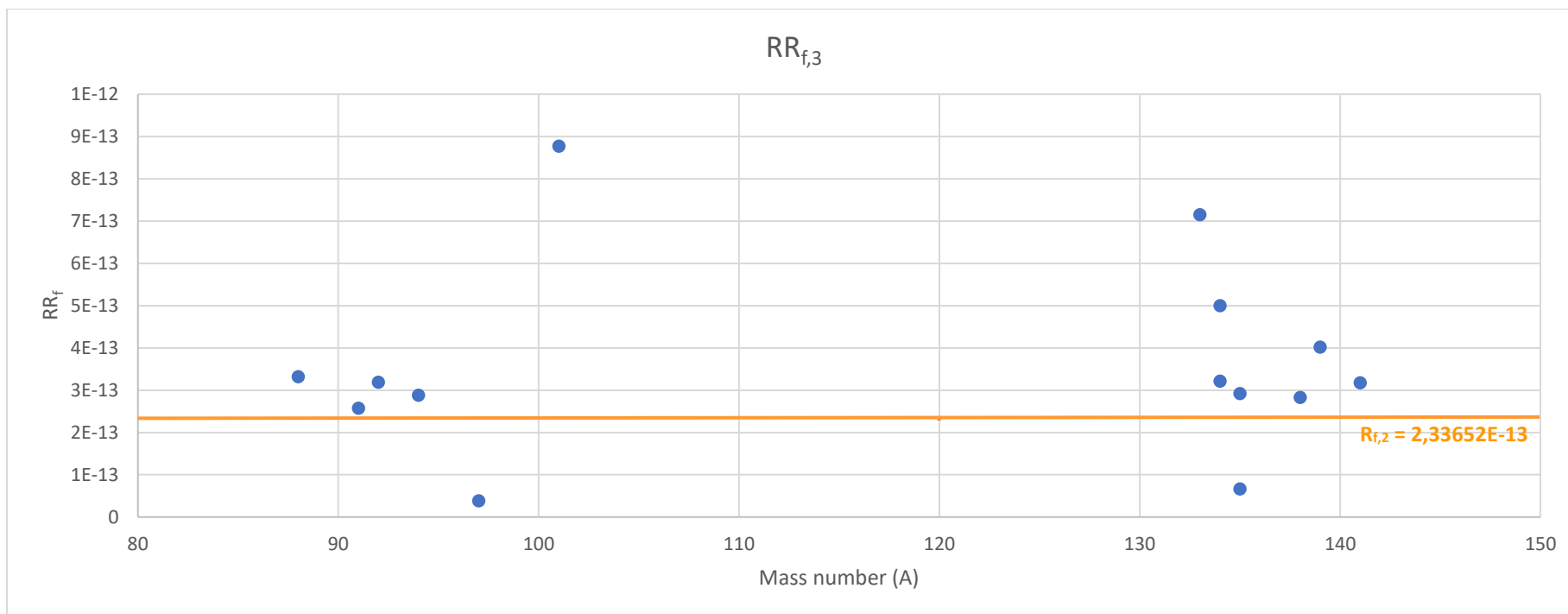
Irradiation time	900 s	Effectivity for 30 mm distance		Self-shielding correction	
Irradiation end	10:36:00 (12/04/2019)	koef	err	Product	Energy [MeV] MAC [cm ² /g]
Acquisition time	11:04:29 (12/04/2019)	a=	-5,03255059	Tc101	0,30713 0,4941
Live time	6294,9 s	b=	-0,92597209	Te133	0,31232 0,4771
Real time	6492,8 s	c=	0,02676303		0,19067 1,4540
Dead time	3,05 %	d=	0,01240589	Ba141	0,30455 0,5030
Distance	30 mm	e=	0,01879813		0,27793 0,6122
Cooling time	1709 s	f=	-0,01512472	Te134	0,21077 1,1470
Sample's weight	0,1481 g	g=	-0,01691282		0,27793 0,6122
Number of target nuclei	1,13857E+18	h=	-0,00190221	Ba139	0,16623 2,0200
d	2,83E-02 cm	i=	0	Xe135	0,25012 0,7737
ρ	1,91E+01 g/cm ³	j=	0	Kr88	0,19663 1,3510

Product	Yield	T1/2 [s]	λ	Pk	Energy	Energy correction	Area	%err	Intensity	Effectivity	Saturated activity	Reaction rate	Deviation σ _i	Dev. σ _i [%]
Nb97	0,059968	4326	0,00016023	144	657,97		4969,00	2,20	98,00	0,009653082	1314,50067	3,85045E-14	8,471E-16	2,20
			0,00022131	173	846,84		42525,00	0,50	95,40	0,007612869	14170,67309			
I134	0,0782964	3132	0,00022131	180	883,91		28616,00	0,60	64,90	0,0073145	14588,89835	3,21442E-13	1,22603E-15	0,38
			0,00022131	207	1072,41		5186,00	3,20	14,90	0,006114157	13776,93351			
Tc101	0,0517255	853,2	0,00081241	71	307,13	1,1392	63082,00	0,50	89,00	0,020423218	22591,12863			
			0,00081241	120	545,09		3290,00	3,10	5,96	0,011555684	31095,72157	8,77185E-13	4,33157E-15	0,49
			0,00034578	235	1436,02		20899,00	0,90	76,30	0,004685159	15745,85237			
Cs138	0,0670757	2004,6	0,00034578	105	462,86		7601,00	2,40	30,70	0,013547664	4922,179685	2,82589E-13	1,22603E-15	0,43
			0,00034578	199	1009,49		11840,00	1,10	29,80	0,006465375	16551,26573			
Te133	0,0305767	750	0,0009242	73	312,32	1,1342	17464,00	1,00	62,00	0,020079991	11518,16494			
			0,0009242	90	407,84		4817,00	3,00	27,10	0,015352747	9506,398822	7,15073E-13	2,37631E-15	0,33
Y94	0,064527	1122	0,00061778	187	918,58		9558,00	1,20	56,00	0,007057074	10577,14925	2,87937E-13	3,45525E-15	1,20
			0,00063232	41	190,67	1,4430	18200,00	1,40	46,00	0,032219482	5529,124906			
Ba141	0,0582849	1096,2	0,00063232	70	304,55	1,1418	11133,00	1,90	25,40	0,020598169	9581,009693	3,17459E-13	2,1268E-15	0,67
			0,00063232	64	277,93	1,1742	49831,00	0,90	23,40	0,022588076	42448,84846			
			0,00027637	162	767,06		14290,00	1,80	29,50	0,00835217	14440,46823			
Te134	0,069725	2508	0,00027637	46	210,77	1,3412	32514,00	1,50	22,70	0,029520808	12080,54908	4,99637E-13	3,75265E-15	0,75
			0,00027637	64	277,93	1,1742	49831,00	0,90	21,20	0,022588076	25909,25179			
Ba139	0,064134	4983,6	0,00013909	34	166,23	1,6421	29108,00	0,80	23,7	0,035761587	8931,007206	4,01673E-13	3,21338E-15	0,80
Sr92	0,0593787	9756	7,1048E-05	233	1384,07		13001,00	1,30	90	0,004843439	10781,16919	3,18938E-13	4,14619E-15	1,30



Product	Yield	T1/2 [s]	λ	Pk	Energy	Energy correction	Area	%err	Intensity	Effectivity	Saturated activity	Reaction rate	Deviation σ_i	Dev. σ_i [%]
Xe135	0,065385	32904	2,1066E-05	56	250,12	1,2232	4880,00	7,10	90	0,025086348	2027,86648	6,664E-14	4,73144E-15	7,10
Kr88	0,0355237	10224	6,7796E-05	278	2393,80		1647,00	2,70	34,60	0,002976106	5958,251333	3,31715E-13	4,58008E-15	1,38
			6,7796E-05	44	196,63	1,4084	11006,00	1,60	25,98	0,031391434	5027,2323			
Sr91	0,058275	34668	1,9994E-05	202	1024,10		1794,00	6,50	33,00	0,006380004	8375,004218	2,57497E-13	1,02062E-14	3,96
			1,9994E-05	159	749,62		1773,00	5,00	23,61	0,008534662	8648,164721			
I135	0,0628187	23652	2,9306E-05	223	1260,43		2341,00	5,30	28,9	0,005272552	10824,88376	2,91656E-13	8,52057E-15	2,92
			2,9306E-05	212	1131,42		1930,00	3,50	22,74	0,005820039	10274,99231			

Reaction rate for fission of the third measurement: $RR_{f,3} = 2,33652E-13$; Deviation σ_i : $5,26967E-16$; Deviation σ_i [%]: **0,23%**.



4.4 RESULTS OF THE FOURTH MEASUREMENT

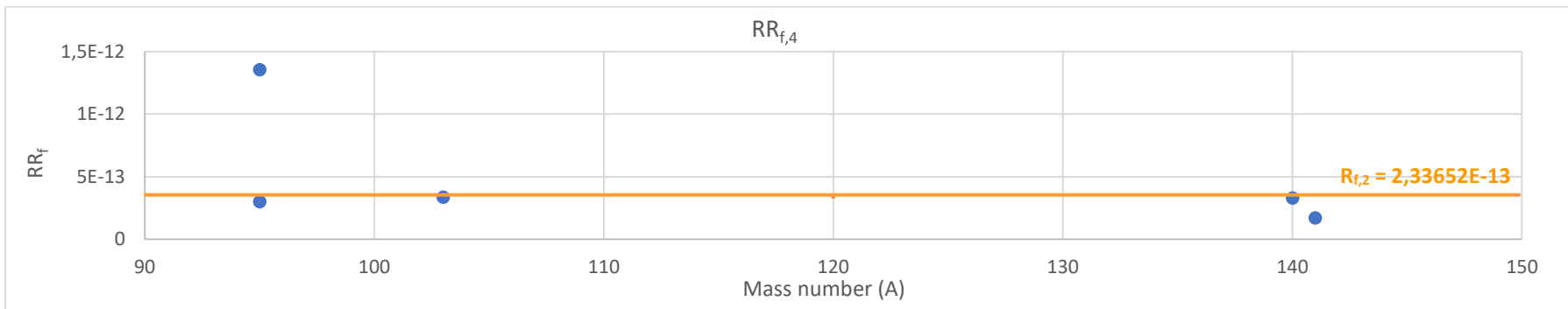
Irradiation time	900	s
Irradiation end	12/04/2019 10:36	(12/04/2019)
Acquisition time	10/05/2019 14:48	(10/05/2019)
Live time	249064,4	s
Real time	249498,7	s
Dead time	0,17	%
Distance	3	mm
Cooling time	2434332	s
Sample's weight	0,1481	g
Number of target nuclei	1,13857E+18	
d	2,83E-02	cm
ρ	1,91E+01	g/cm ³

Effectivity for 3mm distance		
	coef	err
a=	-3,78646607	
b=	-0,93279739	
c=	-0,01086949	
d=	0,01700075	
e=	0,10597276	
f=	0,05205943	
g=	0,00159036	
h=	0	
i=	0	
j=	0	

Self-shielding correction		
Product	Energy [MeV]	MAC [cm ² /g]
Ce141	0,14592	2,77E+00

Product	Yield	T1/2 [s]	λ	Pk	Energy	Energy correction	Area	%err	Intensity	Effectivity	Saturated activity	Reaction rate	Deviation σ_i	Dev. σ_i [%]
Nb95	0,0650287	3021840	2,2938E-07	67	766,3		41634	0,8	100	0,029048153	50134,63693	1,35426E-12	1,08341E-14	0,80
Ru103	0,0303093	3392064	2,0434E-07	49	497,26		6248	4,9	90,9	0,043756717	5785,173055	3,35283E-13	1,64288E-14	4,90
Zr95	0,0650274	5531328	1,2531E-07	66	756,69		3896	6,2	54	0,029391181	12043,06273	3,00892E-13	1,42658E-14	4,74
			1,2531E-07	61	724,17		2821	7,3	44,17	0,030618232	10233,50407			
Ce141	0,0584699	2808086,4	2,4684E-07	28	145,92	1,9273	10901	2,7	48,2	0,136353114	5637,688343	1,69371E-13	4,57302E-15	2,70
Ba140	0,0621448	1101772,8	6,2912E-07	52	537,42		3257	9,9	24,39	0,040581528	11664,54547	3,29711E-13	3,26414E-14	9,90

Reaction rate for fission of the fourth measurement: $RR_{f,4} = 3,43984E-13$; Deviation σ_i : $3,8956E-15$; Deviation σ_i [%]: 1,13%.

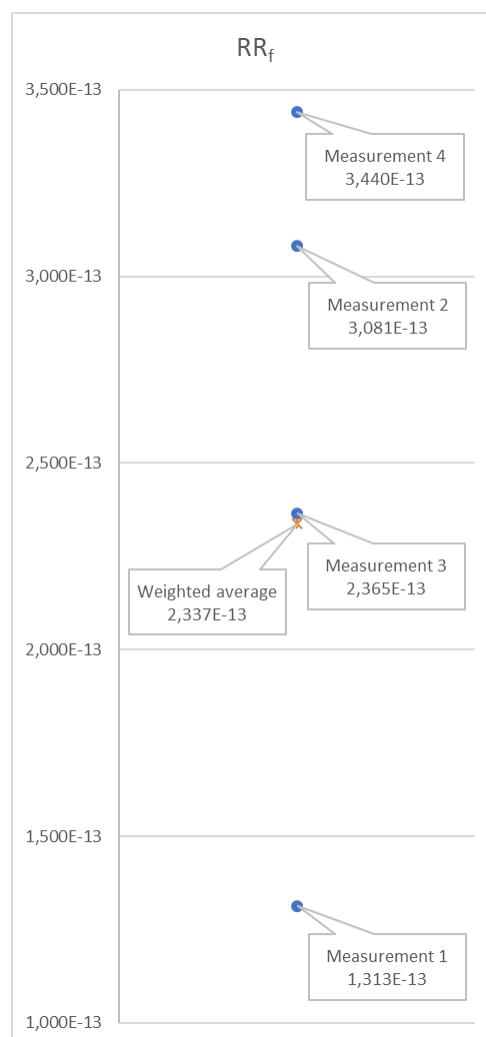


5 DISCUSSION

5.1 REACTION RATE FOR FISSION

Analyzing the results of the Reaction Rate for fission of the four measurements, it can be observed that they are all the same order of magnitude. If the weighted average is calculated, one can see that measurement 2 and 3 are closer to this average while measurement 1 and 4 are a bit further, being measurement 1 the one that is furthest. Nevertheless, all the deviations are below 2%, which means that the values are very close to the weighted average and to each other.

Measurement	RR _f	Dev. σ _i [%]
Nº 1	1,313E-13	1,68
Nº 2	3,081E-13	0,55
Nº 3	2,337E-13	0,23
Nº 4	3,440E-13	1,13
Weighted average	2,365E-13	-



Being the reaction rate the number of interactions taking place in a cubic centimeter in one second, one can observe that the number of this interactions has been more or less increasing in time because, as the graphic above shows, the lowest value of RR_f was measured in the first measurement and the highest was measured in the last measurement (measurement 4).

5.2 REACTION RATE FOR FISSION AND REACTION RATE FOR NEUTRON CAPTURE

To obtain the reaction rate for neutron capture we first need to calculate the Reaction rate for U²³⁹.

Nuclide	A	E _γ [keV]	I _γ [%]
U239	239	74,6641	48

Self-shielding correction		
Measurement	Energy [MeV]	MAC [cm ² /g]
1	0,07508	3,981
2	0,07507	3,982
3	0,07508	3,981



	Pk	Energy	Self-shield. corr.	Area	%err	Effectivity	Saturated activity	Reaction rate	σ_i
Measurement 1	2	75,08	2,4319	9191	1,5	0,00396049	38121,39169	2,47E-16	3,71084E-18
Measurement 2	2	75,07	2,43	149598	0,3	0,00770551	216937,2177	1,40807E-15	4,22421E-18
Measurement 3	9	75,08	2,4319	676887,00	0,10	0,00770765	628091,5194	4,07601E-15	4,07601E-18 ²

The formula for calculating the *Reaction Rate for neutron capture* is the following:

$$RR_{\gamma} = \frac{\sum_j \frac{RR_j^{U^{239}}}{\sigma_j}}{\sum_j \frac{1}{\sigma_j}}$$

Where:

$RR_j^{U^{239}}$: Reaction Rate of each one of the measurements “j” from 1 to 3.

σ_j : Deviation of each one of the measurements “j” from 1 to 3.

So, the final value obtained is: **$RR_{\gamma} = 1,86282E - 15$** .

If we now compare the reaction rate for fission with the reaction rate for neutron capture (or absorption):

RR_{γ}	RR_f
1,863E-15	2,365E-13

These two orders of magnitude of difference can be explained by the fact that cross-sections for fission and for neutron absorption of ^{235}U are also different by two orders of magnitude, according to JEFF 3.1 database:

$$U^{235} \begin{cases} \sigma = 584,9 \text{ barns (for **neutron absorption**)} \\ \sigma = 1,21 \text{ barns (for **fission**)} \end{cases}$$

5.3 COMPARISON WITH RESULTS FROM MCNP

In this section the results are compared with the ones calculated by *MCNP code* (<https://mcnp.lanl.gov/>) version 6 with cross section library B-7. The uranium foil was modelled as a uranium cylinder inside a plastic capsule.

² The fourth measurement is not included in this analysis because the half-life of U^{239} is only 23,45 min, so there is no chance to find this nuclide in the fourth measurement.



MCNP calculated values	
RR_f	σ [%]
2,723E-05	0,57
RR_γ	σ [%]
8,559E-05	2,55

The final value for both reaction rates from MCNP was calculated by following formula:

$$Final\ RR = \frac{RR * Reactor\ power\ normalisation\ constant}{Number\ of\ nuclei}$$

Reactor power	Reactor power normalization constant		Number of nucleus
1,00E+08	6,39E+12	total	4,83197E+22
1,00E+07	6,39E+11	U235	1,44959E+20
		U238	4,68701E+22

With all this data, the final RR_f and RR_γ can be computed:

Final RR_f	σ
1,1998E-13	6,83889E-16
Final RR_γ	σ
1,16628E-15	2,97402E-17

Now these values can be compared with the ones obtained in the present thesis. Both values are from the same order of magnitude. So MCNP confirms the experimental results obtained through all these experiments.

	Present thesis	MCNP calculation
RR_f	2,365E-13	1,200E-13
RR_γ	1,863E-15	1,166E-15



6 CONCLUSION

Nuclear fission splits a heavy nucleus such as uranium into two lighter nuclei, which are called *fission products*. Yield refers to the fraction of a fission product produced per each fission.

Yield can be categorized by:

- “Chain yield”: Nuclei of a given mass number (A) regardless of atomic number (Z) that represent a decay chain of beta decay.
- Chemical elements spanning various isotopes of same atomic number (Z) but different mass number (A).
- Individual isotopes.

Isotope and element yields will change as the fission products undergo beta decay, while chain yields do not change after completion of neutron emission by a few neutron-rich initial fission products (delayed neutrons), with half-life measured in seconds.

A few isotopes can be produced directly by fission, but not by beta decay because the would-be precursor with atomic number one greater is stable and does not decay. Chain yields do not account for these "shadowed" isotopes; however, they have very low yields (less than a millionth as much as common fission products) because they are far less neutron-rich than the original heavy nuclei.

One of the main goals of this thesis was to study the distribution of fission products, so in the following table one can find a summary of the products found on each measurement:

1st measurement	2nd measurement	3rd measurement	4th measurement
I134	I134	I134	Ba140
Tc101	Tc101	Tc101	Ce141
Te133	Te133	Te133	Nb95
Y94	Y94	Y94	Ru103
Rb89	Rb89	Xe135	Zr95
Sr93	Sr93	I135	
Xe138	Xe138	Kr88	
Ce145	Ba139	Ba139	
Rb90	Ba141	Ba141	
Sr94	Cs138	Cs138	
Xe137	Te134	Te134	
	La142	Nb97	
		Sr91	
		Sr92	



Highlighted in orange one can find the nuclides that were present in the first, second and third measurements. In yellow the ones that appeared in both the first and the second measurement. And finally, the elements that were found in the second and third experiment are highlighted in blue.

Since the fourth measurement happened about one month after the other ones, it was foreseeable that the nuclides present in the three first measurements after so much time wouldn't appear in the fourth measurement. That's why none of the nuclides present in the fourth measurement are highlighted.

The present thesis gives many measured data and analysis in detail of fission yield measurements from uranium irradiated in the VR-1 reactor. Since many measurements were performed and results were verified in MCNP code this thesis can be used as a basis for future experiments. This work has given an experimental verification of some basic laws known from reactor physics and also verified the theoretical values of constant Reaction Rate for fission and Reaction Rate for neutron capture.

For more details about the nuclide library used for identification of nuclides or about gamma-spectrometries for the four measurements, see Appendixes 1 and 2.



7 REFERENCES

- [1] J. R. Lamarsh y A. J. Baratta, *Introduction to Nuclear Engineering*, Upper Saddle River, New Jersey: Prentice-Hall, Inc., 2001.
- [2] International Atomic Energy Agency (IAEA), «Compilation and evaluation of fission yield nuclear data,» Nuclear Data Section, Vienna, 2000.
- [3] Z. B. Alfassi, «Instrumental Neutron Activation Analysis,» John Wiley & Sons Ltd, Beer Sheva, Israel, 2000.
- [4] Z. B. Alfassi, *Activation Analysis Volume I*, Boca Raton, Florida: CRC Press, Inc., 1990.
- [5] P. Bode, A. Byrne, Z. Chai, A. Chatt, V. Dimic, T. Hossain, J. Kučera, G. Lalor y R. Parthasarathy, «Use of research reactors for neutron activation analysis,» 2001.
- [6] Z. B. Alfassi, *Activation Analysis Volume II*, Boca Raton, Florida: CRC Press, Inc., 1990.
- [7] N. Reguigui, «Gamma Ray Spectrometry. Practical information,» 2006.
- [8] G. F. Knoll, *Radiation detection and measurement*, Hoboken, New Jersey: John Wiley & Sons, 2010.
- [9] N. Soppera, «JANIS 4.0,» OECD / NEA Data Bank, 17 February 2019. [En línea]. Available: <https://www.oecd-nea.org/janis/>. [Último acceso: 14 April 2019].
- [10] S. Y. F. Chu, L. Ekström y R. B. Firestone, «Decay data search,» LBNL, Berkeley, USA; Department of Physics, Lund University, Sweden, 29 April 1998. [En línea]. Available: <http://nucldata.nuclear.lu.se/toi/nucSearch.asp>. [Último acceso: 24 May 2019].



APPENDIX 1: NUCLIDE LIBRARY

Product	Yield	Error	T1/2	Time unit	Eg (keV)	Ig (%)	Eg (keV)	Ig (%)	Eg (keV)	Ig (%)
Nb97	0,059968	5,9968	72,1	m	658,08	98				
I134	0,0782964	0,00469778	52,2	m	847,025	95,4	884,09	64,9	1072,55	14,9
Nb95	0,0650287	91,0401	34,975	d	765,794	100				
Zr98	0,0563561	0,0129619	30,7	s	2250	100				
La140	0,0621969	62,1969	1,6781	d	1596,21	95,4	487,021	45,5	815,772	23,28
I132	0,0431185	0,0275959	2,295	h	667,718	99	772,6	75,6	954,55	17,6
Tc101	0,0517255	72,4157	14,22	m	306,857	89	545,117	5,96		
Cs137	0,0618832	30,9416	30,07	y	661,657	85,1				
La144	0,0546501	76,5101	40,8	s	395,44	94,3	541,2	39,2	844,8	22,3
Zr97	0,059836	0,00119672	16,91	h	743,36	93	507,64	5,03		
Xe135	0,065385	45,7695	9,14	h	249,77	90				
Cs138	0,0670757	4,6953	33,41	m	1435,795	76,3	462,796	30,7	1009,78	29,8
Sr92	0,0593787	83,1301	2,71	h	1383,93	90				
Mo99	0,0610873	85,5223	65,94	h	140,511	89,43	739,5	12,13	181,063	5,99
Sr93	0,0623749	62,3749	7,423	m	590,238	68	875,73	24,5	888,13	22,1
Sr94	0,0606287	84,8801	75,3	s	1427,7	94				
Xe139	0,0503877	0,00100775	39,68	s	218,59	56	296,53	21,7	174,97	11,3
Ru103	0,0303093	42,4331	39,26	d	497,08	90,9	610,33	5,75		
Te133	0,0305767	85,6147	12,5	m	312,072	62	407,63	27,1	1333,21	10,67
Cs140	0,0572416	80,1382	63,7	s	602,35	52,5	908,25	8,56		
I133	0,0669654	0,0428578	20,8	h	529,872	87				
Te132	0,042948	60,1272	3,204	d	228,16	88	49,72	15		
Ce145	0,0393304	0,00235982	3,01	m	724,33	59	62,54	13,33	1148,03	9,15
Rb90	0,0449896	62,9854	158	s	831,69	39,9	1060,7	9,5		
Rb89	0,0471522	66,0131	15,15	m	1031,94	58	1248,19	42,6	2196,02	13,3



Product	Yield	Error	T1/2	Time unit	Eg (keV)	Ig (%)	Eg (keV)	Ig (%)	Eg (keV)	Ig (%)
Y94	0,064527	6,4527	18,7	m	918,74	56	1138,88	6	550,88	4,9
Kr90	0,0486298	68,0817	32,32	s	1118,69	39	121,82	35,5	539,49	30,8
Zr95	0,0650274	91,0383	64,02	d	756,729	54	724,199	44,17		
Ce143	0,0595576	83,3806	33,039	h	293,266	42,8				
Kr88	0,0355237	71,0475	2,84	h	2392,11	34,6	196,301	25,98	2195,842	13,18
Sr95	0,0527009	73,7812	23,9	s	685,6	23	2717,3	4,6		
Te135	0,0333923	0,00133569	19	s	603,5	37	266,8	10,36	870,3	7,73
La142	0,0584862	81,8806	91,1	m	641,285	47	2397,8	13,3	2542,7	10
Ba141	0,0582849	0,00163198	18,27	m	190,328	46	304,194	25,4	276,948	23,4
Ce141	0,0584699	58,4699	32,501	d	145,4405	48,2				
Xe138	0,0629685	88,1559	14,08	m	258,411	31,5	434,562	20,3	1768,26	16,7
Xe137	0,0612832	61,2832	3,818	m	455,49	31				
Te134	0,069725	0,0019523	41,8	m	767,2	29,5	210,465	22,7	277,951	21,2
Ba143	0,0554495	0,00155259	14,33	s	211,475	25	798,79	15,6	980,45	11,55
Xe133	0,0669909	0,0428742	5,243	d	80,9971	38				
Sr91	0,058275	5,8275	9,63	h	1024,3	33	749,8	23,61	652,9	8
Ba139	0,064134	44,8938	83,06	m	165,864	23,7				
Rb88	0,0357468	50,0455	17,78	m	1836,063	21,4	898,042	14,04		
Xe140	0,0365384	73,0768	13,6	s	805,52	20	1413,66	12,2	1315,05	8,2
Ba144	0,0439527	87,9053	11,5	s	103,855	23,3	430,48	18,3	172,828	15,4
Ba142	0,057521	0,00115042	10,6	m	255,3	20,5	1204,3	14,23	895,2	13,9
Kr89	0,0451068	63,1495	3,15	m	220,948	20,1	586,03	16,6	904,27	7,2
Ba140	0,0621448	62,1448	12,752	d	537,261	24,39	29,96	14,1	162,66	6,22
I135	0,0628187	87,9461	6,57	h	1260,409	28,9	1131,511	22,74	1678,027	9,62
Kr91	0,0335106	33,5106	8,57	s	108,788	43,5	506,592	19,1	612,87	7,7



APPENDIX 2: GAMMA-SPECTROMETRY RESULTS

MEASUREMENT 1

	Pk	IT	Energy	Area	Bkgnd	FWHM	Channel	Left	PW	Cts/Sec	%err	Fit
	1	0	25,35	538	697	0,37	144,04	140	10	1,30E+00	9,3	0
	2	0	75,08	9191	3244	0,94	425,28	416	18	2,20E+01	1,5	0
	3	0	95,05	1299	3013	0,83	538,23	530	19	3,10E+00	8,3	0
	4	0	98,83	2413	3212	1,03	559,6	548	20	5,80E+00	4,8	0
	5	0	111,55	1222	3363	1,3	631,55	619	23	2,90E+00	9,8	0
	6	0	114,98	413	2820	0,71	650,93	642	20	9,90E-01	24,6	0
	7	0	168,87	334	2892	1,12	955,72	947	22	8,00E-01	31,7	0
M	8	6	181,36	163	1969	0,89	1026,3	1002	39	3,90E-01	22,6	0,7
m	9	6	182,78	198	1843	0,89	1034,38	1002	39	4,70E-01	19,6	0,7
	10	0	190,62	367	2134	0,75	1078,68	1071	14	8,80E-01	21,6	0
	11	0	210,92	366	3177	1,02	1193,49	1184	27	8,70E-01	32,7	0
M	12	5	218,73	363	2258	1,12	1237,64	1227	34	8,70E-01	12,1	0,4
m	13	5	221,32	348	2041	1,13	1252,29	1227	34	8,30E-01	12,3	0,4
	14	0	232	287	1567	1,16	1312,71	1306	16	6,90E-01	24,6	0
M	15	8	255,58	364	1633	0,84	1446,06	1437	35	8,70E-01	10,2	3,3
m	16	8	258,74	573	1733	0,84	1463,94	1437	35	1,40E+00	7,5	3,3
	17	0	277,62	911	1673	1,91	1570,69	1560	23	2,20E+00	9,4	0
M	18	5	301,99	410	1183	1,16	1708,51	1702	50	9,80E-01	8,7	0,9
m	19	5	304,52	575	1448	1,17	1722,82	1702	50	1,40E+00	6,7	0,9
m	20	5	307,09	1107	1428	1,17	1737,38	1702	50	2,60E+00	4,2	0,9
M	21	4	312,31	1131	1097	1,12	1766,86	1759	49	2,70E+00	4	0,7
m	22	4	314,81	298	1189	1,12	1781,01	1759	49	7,10E-01	10,6	0,7



	Pk	IT	Energy	Area	Bkgnd	FWHM	Channel	Left	PW	Cts/Sec	%err	Fit
m	23	4	317,08	782	1161	1,12	1793,85	1759	49	1,90E+00	5,1	0,7
M	24	8	343,85	371	1206	1,15	1945,26	1934	38	8,90E-01	9,5	1
m	25	8	346,49	234	1167	1,15	1960,17	1934	38	5,60E-01	13,7	1
	26	0	358,17	812	1565	0,99	2026,26	2011	28	1,90E+00	10,9	0
	27	0	364,26	202	1031	0,89	2060,69	2053	20	4,80E-01	30,5	0
	28	0	397,26	338	1463	0,56	2247,28	2234	29	8,10E-01	24,9	0
	29	0	402,51	194	1151	0,92	2277,02	2264	22	4,60E-01	34,7	0
	30	0	407,75	801	1521	1,15	2306,6	2294	29	1,90E+00	11,1	0
	31	0	411,94	125	767	0,71	2330,34	2322	17	3,00E-01	40,3	0
	32	0	434,85	866	1365	1,31	2459,86	2450	26	2,10E+00	9,4	0
M	33	7	453,85	200	848	1,09	2567,32	2559	28	4,80E-01	13,6	1,4
m	34	7	455,55	722	1094	1,09	2576,96	2559	28	1,70E+00	5,6	1,4
	35	0	462,72	612	1294	1,37	2617,49	2601	31	1,50E+00	13,6	0
	36	0	467,22	170	708	0,53	2642,96	2635	16	4,10E-01	28,2	0
	37	0	474,95	190	839	0,39	2686,64	2675	22	4,50E-01	30,5	0
	38	0	497,48	108	1022	0,5	2814,09	2801	24	2,60E-01	59,9	0
	39	0	506,18	186	814	1,06	2863,28	2851	21	4,40E-01	30,1	0
	40	0	510,82	473	1257	1,98	2889,52	2876	30	1,10E+00	17	0
M	41	6	530,55	148	779	1,47	3001,07	2993	44	3,50E-01	19,3	0,7
m	42	6	534,99	125	830	1,47	3026,18	2993	44	3,00E-01	21,7	0,7
	43	0	554,73	72	590	0,39	3137,86	3131	17	1,70E-01	61,1	0
	44	0	566,14	303	815	0,26	3202,33	3191	25	7,20E-01	20	0
	45	0	577,56	248	777	1,04	3266,97	3257	26	5,90E-01	24	0
M	46	4	585,94	354	675	1,47	3314,35	3304	53	8,50E-01	8,2	0,8
m	47	4	590,32	2118	751	1,48	3339,1	3304	53	5,10E+00	2,5	0,8
	48	0	602,31	292	852	1,4	3406,93	3399	26	7,00E-01	21,4	0
	49	0	621,43	219	698	0,66	3515,04	3500	25	5,20E-01	25,5	0



	Pk	IT	Energy	Area	Bkgnd	FWHM	Channel	Left	PW	Cts/Sec	%err	Fit
	50	0	636,11	138	651	0,73	3598,04	3587	23	3,30E-01	37,3	0
	51	0	641,73	427	927	1,89	3629,83	3612	31	1,00E+00	16,5	0
	52	0	647,77	246	441	1,14	3663,98	3656	17	5,90E-01	16,4	0
	53	0	657,78	144	657	0,83	3720,62	3712	21	3,40E-01	34,9	0
	54	0	696,92	884	919	1,43	3941,95	3924	34	2,10E+00	8,5	0
	55	0	710,18	420	578	1,12	4016,94	4007	20	1,00E+00	11,8	0
	56	0	724,11	786	808	1,54	4095,73	4081	33	1,90E+00	8,9	0
M	57	5	738,78	95	606	1,51	4178,66	4169	48	2,30E-01	24,2	1
m	58	5	742,77	307	662	1,52	4201,26	4169	48	7,30E-01	9,5	1
	59	0	759,69	67	339	0,84	4296,94	4289	18	1,60E-01	51	0
	60	0	767,19	333	627	0,46	4339,34	4326	28	7,90E-01	16,9	0
	61	0	779,96	80	519	0,64	4411,58	4401	21	1,90E-01	55,3	0
	62	0	793,3	634	508	1,33	4487,02	4473	29	1,50E+00	8,6	0
	63	0	816,51	217	569	0,42	4618,26	4606	27	5,20E-01	24	0
	64	0	823,88	89	401	0,32	4659,95	4650	23	2,10E-01	45,4	0
	65	0	831,35	874	522	1,34	4702,21	4685	30	2,10E+00	6,6	0
M	66	5	839,37	636	455	1,44	4747,55	4738	70	1,50E+00	5,1	0,9
m	67	5	843,94	150	446	1,44	4773,37	4738	70	3,60E-01	13,7	0,9
m	68	5	846,89	298	417	1,44	4790,06	4738	70	7,10E-01	8,1	0,9
	69	0	875,78	549	405	1,56	4953,49	4940	27	1,30E+00	8,8	0
M	70	7	883,93	160	490	1,5	4999,53	4987	48	3,80E-01	13,7	1,1
m	71	7	888,05	427	404	1,51	5022,85	4987	48	1,00E+00	6,6	1,1
	72	0	894,74	234	424	1,04	5060,7	5043	27	5,60E-01	19,5	0
	73	0	912,37	205	370	0,74	5160,39	5148	24	4,90E-01	20,1	0
	74	0	918,63	732	535	1,57	5195,76	5181	32	1,70E+00	8	0
	75	0	933,23	191	394	0,8	5278,33	5266	26	4,60E-01	22,6	0
M	76	5	943,12	277	353	1,96	5334,26	5322	58	6,60E-01	8,7	1,1



	Pk	IT	Energy	Area	Bkgnd	FWHM	Channel	Left	PW	Cts/Sec	%err	Fit
m	77	5	948,21	365	378	1,97	5363,09	5322	58	8,70E-01	7,1	1,1
	78	0	953,44	376	258	1,49	5392,62	5381	27	9,00E-01	10,3	0
	79	0	974,07	680	312	1,55	5509,29	5497	28	1,60E+00	6,7	0
	80	0	1000,73	149	260	0,42	5660,08	5649	22	3,60E-01	22,5	0
M	81	19	1012,19	50	318	1,11	5724,88	5718	49	1,20E-01	80,8	1,2
m	82	19	1017,59	45	280	1,11	5755,42	5718	49	1,10E-01	80,9	1,2
	83	0	1031,78	706	383	1,78	5835,7	5822	31	1,70E+00	7,2	0
	84	0	1078,68	189	240	1,7	6100,93	6089	24	4,50E-01	17,9	0
	85	0	1095,83	125	274	0,59	6197,93	6187	24	3,00E-01	27,9	0
	86	0	1147,93	74	174	0,56	6492,55	6484	18	1,80E-01	34,2	0
	87	0	1161,16	115	191	1,88	6567,39	6555	26	2,70E-01	26,6	0
	88	0	1204,11	176	270	1,27	6810,26	6799	24	4,20E-01	20,1	0
	89	0	1248,18	445	287	0,92	7059,45	7042	33	1,10E+00	9,8	0
	90	0	1283,29	101	170	0,55	7258,06	7249	22	2,40E-01	26,9	0
	91	0	1312,97	163	149	0,48	7425,86	7414	24	3,90E-01	17	0
M	92	7	1321,19	77	161	1,8	7472,34	7462	37	1,80E-01	18,8	1,2
m	93	7	1323,93	120	152	1,8	7487,87	7462	37	2,90E-01	13,3	1,2
	94	0	1333,23	93	90	0,56	7540,46	7531	19	2,20E-01	21,5	0
	95	0	1383,85	128	181	0,27	7826,71	7815	25	3,10E-01	23,2	0
	96	0	1427,91	319	101	1,44	8075,92	8063	27	7,60E-01	8,7	0
	97	0	1435,99	384	125	1,34	8121,62	8109	30	9,20E-01	8,2	0
	98	0	1525,38	68	64	0,26	8627,09	8618	20	1,60E-01	24,9	0
	99	0	1533,34	39	135	0,3	8672,13	8663	20	9,20E-02	58,7	0
	100	0	1694,46	61	80	0,24	9583,32	9574	20	1,50E-01	30,2	0
	101	0	1769,04	210	66	0,28	10005	9993	26	5,00E-01	10,5	0
	102	0	2005,85	69	41	0,22	11344,3	11333	22	1,60E-01	21,6	0
	103	0	2016,93	138	36	0,67	11406,9	11395	25	3,30E-01	12,3	0



	Pk	IT	Energy	Area	Bkgnd	FWHM	Channel	Left	PW	Cts/Sec	%err	Fit
	104	0	2033,13	43	49	0,36	11498,5	11489	20	1,00E-01	34,4	0
	105	0	2176,81	92	25	0,31	12311,1	12301	22	2,20E-01	14,8	0
	106	0	2197,32	94	30	0,25	12427,1	12417	22	2,20E-01	15,3	0
	107	0	2572,03	37	31	0,8	14546,1	14536	22	8,80E-02	34,4	0
	108	0	2650,76	17	9	0,27	14991,4	14981	22	4,20E-02	41,1	0

MEASUREMENT 2

	Pk	IT	Energy	Area	Bkgnd	FWHM	Channel	Left	PW	Cts/Sec	%err	Fit
	1	0	25,36	2207	2556	0,42	144,1	140	9	2,40E+00	4,3	0
M	2	12	75,07	149598	12980	0,94	425,25	414	50	1,60E+02	0,3	2,2
m	3	12	78,09	650	9798	0,95	442,3	414	50	7,10E-01	12,3	2,2
m	4	12	79,88	1372	9545	0,95	452,43	414	50	1,50E+00	6,2	2,2
	5	0	87,04	288	8086	0,55	492,93	487	14	3,20E-01	52,3	0
	6	0	95,06	15574	12201	0,99	538,3	530	18	1,70E+01	1,5	0
M	7	32	98,84	28915	12028	1,03	559,68	548	62	3,20E+01	0,7	3,1
m	8	32	101,37	430	10334	1,03	573,94	548	62	4,70E-01	18,3	3,1
m	9	32	104,15	613	10487	1,03	589,66	548	62	6,70E-01	13,1	3,1
m	10	32	106,55	768	8543	1,04	603,28	548	62	8,40E-01	10,6	3,1
M	11	9	110,83	3932	9131	0,98	627,48	619	24	4,30E+00	4,3	1,1
m	12	9	111,72	7241	9407	0,98	632,49	619	24	8,00E+00	2,7	1,1
M	13	6	114,98	3688	9714	1,13	650,92	642	33	4,10E+00	3	1,5
m	14	6	118,1	425	7113	1,14	668,57	642	33	4,70E-01	16,9	1,5
	15	0	128,03	960	9048	1,32	724,73	712	24	1,10E+00	20,1	0
	16	0	143,77	293	4632	0,8	813,74	809	12	3,20E-01	37,2	0



	Pk	IT	Energy	Area	Bkgnd	FWHM	Channel	Left	PW	Cts/Sec	%err	Fit
M	17	8	148,66	388	6089	1,08	841,4	835	48	4,30E-01	19	0,7
m	18	8	150,08	3307	7184	1,08	849,46	835	48	3,60E+00	3,2	0,7
m	19	8	151,67	710	7122	1,08	858,41	835	48	7,80E-01	9,9	0,7
m	20	8	154,22	966	7415	1,08	872,85	835	48	1,10E+00	7,6	0,7
M	21	5	166,21	1707	7097	1,04	940,66	931	38	1,90E+00	4,7	0,6
m	22	5	168,94	1900	6496	1,05	956,09	931	38	2,10E+00	4,3	0,6
	23	0	177,35	271	5030	0,75	1003,64	997	15	3,00E-01	44,9	0
M	24	4	181,22	2476	6478	1,01	1025,52	1012	32	2,70E+00	3,4	0,7
m	25	4	182,66	1545	6291	1,01	1033,66	1012	32	1,70E+00	4,8	0,7
M	26	4	190,68	7821	5691	1,05	1079,03	1067	36	8,60E+00	1,4	0,8
m	27	4	192,37	2879	5913	1,05	1088,62	1067	36	3,20E+00	2,8	0,8
	28	0	196,5	1194	7206	1,01	1111,93	1102	24	1,30E+00	14,5	0
	29	0	201,57	1236	6490	0,67	1140,63	1132	22	1,40E+00	13	0
M	30	8	210,8	3669	5381	1,08	1192,8	1179	29	4,00E+00	4,1	1,4
m	31	8	211,86	695	5494	1,08	1198,84	1179	29	7,60E-01	16,9	1,4
M	32	5	218,64	1523	4656	0,97	1237,17	1229	31	1,70E+00	4,8	1,2
m	33	5	221,23	483	4501	0,97	1251,8	1229	31	5,30E-01	11,8	1,2
M	34	5	225,67	180	4479	0,97	1276,94	1269	54	2,00E-01	29,5	0,8
m	35	5	228,48	562	4652	0,97	1292,78	1269	54	6,20E-01	10	0,8
m	36	5	231,94	1662	4276	0,98	1312,38	1269	54	1,80E+00	4,4	0,8
	37	0	242,91	529	4596	1,16	1374,4	1365	19	5,80E-01	23,9	0
M	38	30	255,59	2624	4393	1,06	1446,13	1436	73	2,90E+00	2,9	1,6
m	39	30	258,69	5373	4270	1,06	1463,67	1436	73	5,90E+00	1,7	1,6
m	40	30	260,31	769	4195	1,07	1472,79	1436	73	8,50E-01	7,3	1,6
m	41	30	264,84	515	4085	1,07	1498,4	1436	73	5,70E-01	10,6	1,6
	42	0	277,65	6961	5756	1,81	1570,89	1556	30	7,70E+00	2,7	0
M	43	4	304,47	3368	3505	1,11	1722,54	1707	46	3,70E+00	2,3	1,2



	Pk	IT	Energy	Area	Bkgnd	FWHM	Channel	Left	PW	Cts/Sec	%err	Fit
m	44	4	307,11	11439	3405	1,11	1737,5	1707	46	1,30E+01	1,1	1,2
M	45	5	312,31	5410	3354	1,16	1766,9	1757	51	6,00E+00	1,7	0,9
m	46	5	314,89	1146	3333	1,16	1781,45	1757	51	1,30E+00	4,8	0,9
m	47	5	317,04	3243	3201	1,16	1793,64	1757	51	3,60E+00	2,3	0,9
M	48	8	331,42	579	4453	1,66	1874,98	1856	54	6,40E-01	10,1	1,5
m	49	8	334,88	786	4146	1,67	1894,52	1856	54	8,70E-01	7,9	1,5
M	50	7	343,9	1892	2838	1,16	1945,52	1931	51	2,10E+00	3,4	0,8
m	51	7	346,69	237	2858	1,16	1961,3	1931	51	2,60E-01	18,1	0,8
m	52	7	348,87	148	2596	1,16	1973,63	1931	51	1,60E-01	28,7	0,8
M	53	6	356,79	300	2807	1,22	2018,44	2008	30	3,30E-01	25,6	0,8
m	54	6	358,1	3712	2861	1,22	2025,85	2008	30	4,10E+00	2,9	0,8
	55	0	364,18	614	2718	1,22	2060,2	2048	22	6,80E-01	16,9	0
	56	0	381,74	166	1714	0,39	2159,55	2153	14	1,80E-01	42,1	0
	57	0	396,7	704	2296	1,05	2244,15	2233	20	7,70E-01	13,3	0
	58	0	402,66	1107	2821	1,42	2277,82	2265	23	1,20E+00	9,9	0
M	59	7	407,87	1766	2569	1,11	2307,33	2298	28	1,90E+00	4,4	0,6
m	60	7	409,13	384	2364	1,11	2314,41	2298	28	4,20E-01	14,3	0,6
	61	0	425,24	503	2324	0,98	2405,52	2393	22	5,50E-01	19,1	0
	62	0	434,9	4270	3326	1,46	2460,15	2444	32	4,70E+00	3,4	0
M	63	6	452,52	520	1851	1,32	2559,82	2551	110	5,70E-01	10,2	1,1
m	64	6	454,04	2069	2106	1,32	2568,38	2551	110	2,30E+00	3,4	1,1
m	65	6	455,73	750	2168	1,32	2577,97	2551	110	8,20E-01	7	1,1
m	66	6	457,67	510	2143	1,32	2588,92	2551	110	5,60E-01	7,8	1,1
m	67	6	461,17	953	2015	1,32	2608,72	2551	110	1,00E+00	5,9	1,1
m	68	6	462,8	2996	2070	1,32	2617,94	2551	110	3,30E+00	2,5	1,1
m	69	6	464,73	413	2036	1,33	2628,84	2551	110	4,50E-01	10	1,1
m	70	6	467,44	701	2006	1,33	2644,2	2551	110	7,70E-01	6,3	1,1



	Pk	IT	Energy	Area	Bkgnd	FWHM	Channel	Left	PW	Cts/Sec	%err	Fit
M	71	6	475,25	499	2083	1,44	2688,38	2675	38	5,50E-01	9,4	1
m	72	6	478,07	161	1794	1,44	2704,31	2675	38	1,80E-01	23,8	1
	73	0	505,96	694	2042	0,76	2862,04	2849	24	7,60E-01	13,6	0
	74	0	510,67	771	2706	1,64	2888,69	2876	30	8,50E-01	15,2	0
M	75	7	526,67	233	1865	1,53	2979,13	2970	46	2,60E-01	17,1	1,2
m	76	7	530,56	597	2157	1,53	3001,13	2970	46	6,60E-01	8,1	1,2
	77	0	535,12	378	1462	1,08	3026,94	3018	19	4,20E-01	19,3	0
M	78	5	541,11	291	1814	1,38	3060,81	3049	103	3,20E-01	13,1	1
m	79	5	545,11	485	1894	1,38	3083,44	3049	103	5,30E-01	8,6	1
m	80	5	546,89	709	1896	1,38	3093,52	3049	103	7,80E-01	6,9	1
m	81	5	550,77	363	1900	1,39	3115,44	3049	103	4,00E-01	10,8	1
m	82	5	554,95	238	1828	1,39	3139,07	3049	103	2,60E-01	15,7	1
	83	0	566,07	1231	2005	1,12	3201,97	3189	27	1,40E+00	8,1	0
	84	0	577,92	488	1660	1,36	3269	3257	24	5,40E-01	17,3	0
	85	0	590,38	4336	2178	1,43	3339,43	3325	29	4,80E+00	2,8	0
	86	0	595,43	420	1634	0,71	3368,03	3356	24	4,60E-01	19,9	0
M	87	32	621,06	569	2413	1,9	3512,96	3496	47	6,30E-01	8,8	1,1
m	88	32	625,32	114	1784	1,9	3537,06	3496	47	1,30E-01	33,3	1,1
	89	0	636,02	178	1087	0,29	3597,55	3589	17	2,00E-01	33,5	0
	90	0	641,44	2491	2356	1,88	3628,22	3610	36	2,70E+00	5	0
	91	0	647,69	782	1564	1,31	3663,55	3653	23	8,60E-01	10,6	0
M	92	6	657,8	776	1551	1,26	3720,74	3708	53	8,50E-01	5,9	1,5
m	93	6	662,17	267	1540	1,26	3745,42	3708	53	2,90E-01	13,1	1,5
	94	0	695,93	737	1888	0,44	3936,35	3922	33	8,10E-01	13,8	0
M	95	6	710,22	761	1393	1,34	4017,16	3999	45	8,40E-01	5,7	1,3
m	96	6	712,97	333	1430	1,35	4032,72	3999	45	3,70E-01	10,8	1,3
M	97	7	719,45	238	1449	1,42	4069,38	4052	53	2,60E-01	14,7	1,2



	Pk	IT	Energy	Area	Bkgnd	FWHM	Channel	Left	PW	Cts/Sec	%err	Fit
m	98	7	724,07	325	1298	1,43	4095,51	4052	53	3,60E-01	11,7	1,2
M	99	9	735,64	160	1330	1,44	4160,95	4151	64	1,80E-01	20,3	1
m	100	9	738,94	211	1420	1,44	4179,59	4151	64	2,30E-01	15,4	1
m	101	9	742,76	1090	1434	1,45	4201,22	4151	64	1,20E+00	4,4	1
	102	0	753,47	283	1217	0,98	4261,78	4249	27	3,10E-01	26,5	0
	103	0	767,09	1602	1526	1,47	4338,8	4322	33	1,80E+00	6,1	0
	104	0	787,65	479	1379	1,72	4455,04	4437	33	5,30E-01	18,2	0
	105	0	793,35	1249	1379	1,39	4487,32	4471	31	1,40E+00	7,1	0
	106	0	812,73	147	868	0,63	4596,92	4585	22	1,60E-01	39,8	0
	107	0	819,2	137	1074	0,36	4633,5	4625	26	1,50E-01	50,2	0
	108	0	824,41	141	767	1,24	4662,94	4652	22	1,50E-01	39	0
M	109	5	831,3	549	972	1,61	4701,9	4689	120	6,00E-01	6,4	1
m	110	5	834,51	187	992	1,62	4720,08	4689	120	2,10E-01	15	1
m	111	5	839,35	1397	994	1,62	4747,42	4689	120	1,50E+00	3,3	1
m	112	5	843,98	525	960	1,62	4773,62	4689	120	5,80E-01	6,5	1
m	113	5	846,83	2063	929	1,62	4789,75	4689	120	2,30E+00	2,6	1
	114	0	857,01	114	701	0,37	4847,29	4837	20	1,30E-01	44,3	0
	115	0	863,79	258	723	1,47	4885,67	4877	22	2,80E-01	21,2	0
M	116	6	871,43	135	919	1,62	4928,88	4919	49	1,50E-01	20,9	1
m	117	6	875,86	1031	948	1,63	4953,92	4919	49	1,10E+00	4,2	1
M	118	6	881,43	450	716	1,57	4985,39	4973	66	5,00E-01	6,9	1,3
m	119	6	883,94	1669	771	1,58	4999,61	4973	66	1,80E+00	2,9	1,3
m	120	6	888,07	777	842	1,58	5022,96	4973	66	8,50E-01	4,8	1,3
	121	0	894,77	824	1026	1,63	5060,86	5042	33	9,10E-01	9,5	0
M	122	5	912,41	887	799	1,62	5160,61	5147	63	9,80E-01	4,8	0,8
m	123	5	914,29	241	829	1,62	5171,25	5147	63	2,70E-01	13,3	0,8
m	124	5	918,56	2809	831	1,63	5195,41	5147	63	3,10E+00	2,1	0,8



	Pk	IT	Energy	Area	Bkgnd	FWHM	Channel	Left	PW	Cts/Sec	%err	Fit
	125	0	925,34	77	482	1,02	5233,75	5225	17	8,40E-02	51,9	0
	126	0	932,73	540	1074	1,51	5275,51	5265	30	5,90E-01	13,9	0
M	127	7	943,06	1037	768	1,8	5333,94	5317	63	1,10E+00	3,9	1,5
m	128	7	948,04	925	853	1,8	5362,11	5317	63	1,00E+00	4,3	1,5
	129	0	953,59	947	846	1,74	5393,48	5380	34	1,00E+00	7,7	0
M	130	6	974,25	221	589	1,31	5510,31	5501	41	2,40E-01	12,3	1,2
m	131	6	978,47	88	495	1,31	5534,2	5501	41	9,70E-02	24,3	1,2
	132	0	1000,78	461	748	1,26	5660,37	5650	28	5,10E-01	13,4	0
M	133	5	1009,5	1087	742	1,64	5709,67	5696	72	1,20E+00	3,8	0,8
m	134	5	1012,21	529	784	1,64	5724,99	5696	72	5,80E-01	6,2	0,8
m	135	5	1017,35	196	829	1,64	5754,07	5696	72	2,20E-01	13,7	0,8
	136	0	1031,7	2634	769	1,67	5835,23	5819	35	2,90E+00	3,1	0
	137	0	1040	151	516	0,24	5882,17	5870	25	1,70E-01	31,6	0
	138	0	1072,34	210	500	0,62	6065,07	6052	25	2,30E-01	22,7	0
	139	0	1078,51	386	577	1,27	6099,97	6084	27	4,20E-01	14	0
	140	0	1093,56	79	486	0,64	6185,06	6174	21	8,70E-02	54,6	0
	141	0	1114,21	137	299	0,37	6301,86	6293	19	1,50E-01	24,8	0
	142	0	1123	305	516	0,61	6351,53	6335	29	3,40E-01	17	0
M	143	8	1136	121	407	1,24	6425,06	6415	56	1,30E-01	16,7	1
m	144	8	1139,04	177	440	1,24	6442,24	6415	56	2,00E-01	12,6	1
m	145	8	1142,17	72	455	1,25	6459,97	6415	56	7,90E-02	26,3	1
	146	0	1160,93	187	424	1,16	6566,08	6555	23	2,10E-01	22,9	0
	147	0	1197,12	77	413	0,43	6770,74	6761	20	8,40E-02	51,2	0
	148	0	1203,98	480	772	1,09	6809,51	6791	36	5,30E-01	14,3	0
	149	0	1248,1	1371	752	1,62	7059,01	7042	32	1,50E+00	5,2	0
M	150	7	1260,7	119	343	1,15	7130,28	7119	39	1,30E-01	16,4	0,6
m	151	7	1263,77	61	285	1,15	7147,65	7119	39	6,70E-02	25,6	0,6



	Pk	IT	Energy	Area	Bkgnd	FWHM	Channel	Left	PW	Cts/Sec	%err	Fit
	152	0	1269,69	114	328	0,39	7181,13	7172	21	1,30E-01	31,7	0
	153	0	1283,26	243	391	0,25	7257,88	7243	30	2,70E-01	18,9	0
	154	0	1323,92	277	378	2,13	7487,82	7472	34	3,00E-01	17,2	0
	155	0	1333,48	179	368	1	7541,86	7525	31	2,00E-01	24,9	0
	156	0	1384,03	633	570	1,08	7827,73	7812	31	7,00E-01	9,2	0
	157	0	1436,05	2051	390	1,64	8121,92	8104	37	2,30E+00	3,2	0
	158	0	1451,73	51	174	0,75	8210,63	8202	19	5,60E-02	49,5	0
	159	0	1525,21	169	252	1,45	8626,13	8611	28	1,90E-01	21,4	0
	160	0	1532,68	129	272	1,11	8668,42	8657	24	1,40E-01	27,2	0
	161	0	1677,67	115	136	0,59	9488,35	9479	21	1,30E-01	21,4	0
	162	0	1769,02	514	220	1,33	10004,9	9987	33	5,70E-01	7,9	0
	163	0	1902,49	68	95	0,38	10759,8	10750	20	7,40E-02	29,7	0
M	164	11	1936,88	24	87	1,09	10954,2	10945	41	2,60E-02	38,2	1
m	165	11	1940,59	36	89	1,09	10975,2	10945	41	4,00E-02	28,6	1
	166	0	2006	87	155	0,99	11345,1	11335	22	9,60E-02	29,7	0
	167	0	2016,99	338	129	0,76	11407,2	11391	33	3,70E-01	9,3	0
	168	0	2033,2	111	129	0,38	11498,9	11488	23	1,20E-01	22,2	0
	169	0	2176,82	149	81	0,7	12311,1	12299	25	1,60E-01	14,7	0
	170	0	2197,36	337	105	1,12	12427,3	12410	35	3,70E-01	8,9	0
	171	0	2219,16	272	73	1,45	12550,6	12538	29	3,00E-01	9,1	0
	172	0	2232,11	40	49	0,24	12623,8	12613	22	4,40E-02	37	0
	173	0	2253,65	65	60	0,68	12745,7	12735	22	7,10E-02	26,4	0
	174	0	2297,52	31	58	0,36	12993,7	12983	22	3,40E-02	52	0
	175	0	2393,87	78	41	0,3	13538,6	13528	22	8,60E-02	19,6	0
	176	0	2544,93	68	37	0,73	14392,9	14382	22	7,50E-02	21,4	0
	177	0	2571,94	176	32	1,59	14545,7	14533	28	1,90E-01	10,2	0
	178	0	2633,84	64	27	0,19	14895,7	14885	22	7,00E-02	20,3	0



	Pk	IT	Energy	Area	Bkgnd	FWHM	Channel	Left	PW	Cts/Sec	%err	Fit
	179	0	2641,23	83	44	0,62	14937,5	14927	22	9,10E-02	19	0
	180	0	2691,34	22	24	0,72	15220,9	15209	24	2,50E-02	48,6	0
	181	0	2709,48	36	17	0,5	15323,5	15312	24	3,90E-02	29,2	0

MEASUREMENT 3

	Pk	Energy	Area	Bkgnd	FWHM	Channel	Left	PW	Cts/Sec	%err	Fit
M	1	25,34	13400,00	6527,00	0,48	143,98	140,00	17,00	2,10	1,00	157,80
m	2	26,02	6964,00	12863,00	0,48	147,83	140,00	17,00	1,10	1,80	157,80
	3	43,81	907,00	37873,00	1,20	248,45	242,00	15,00	0,14	36,60	0,00
	4	63,73	1931,00	38617,00	0,78	361,09	356,00	13,00	0,31	16,70	0,00
M	5	70,04	3359,00	56009,00	0,94	396,77	385,00	79,00	0,53	5,70	2,40
m	6	71,38	6897,00	55716,00	0,95	404,33	385,00	79,00	1,10	3,30	2,40
m	7	72,54	8603,00	55471,00	0,95	410,94	385,00	79,00	1,40	2,90	2,40
m	8	73,60	11543,00	54912,00	0,95	416,90	385,00	79,00	1,80	2,20	2,40
m	9	75,08	676887,00	51419,00	0,95	425,26	385,00	79,00	110,00	0,10	2,40
m	10	78,11	1269,00	47675,00	0,96	442,44	385,00	79,00	0,20	12,80	2,40
m	11	79,88	13968,00	47351,00	0,96	452,40	385,00	79,00	2,20	1,50	2,40
M	12	93,03	10802,00	57479,00	1,01	526,82	514,00	35,00	1,70	1,90	5,30
m	13	95,05	97014,00	62055,00	1,01	538,21	514,00	35,00	15,00	0,40	5,30
M	14	98,83	162041,00	58480,00	0,98	559,58	548,00	66,00	26,00	0,40	4,20
m	15	99,85	23629,00	58398,00	0,99	565,38	548,00	66,00	3,80	1,80	4,20
m	16	101,40	2877,00	54969,00	0,99	574,12	548,00	66,00	0,46	6,40	4,20
m	17	104,15	32696,00	51838,00	0,99	589,69	548,00	66,00	5,20	0,80	4,20
m	18	106,53	43340,00	48427,00	1,00	603,17	548,00	66,00	6,90	0,60	4,20



	Pk	Energy	Area	Bkgnd	FWHM	Channel	Left	PW	Cts/Sec	%err	Fit
M	19	110,83	23394,00	50844,00	1,02	627,44	618,00	24,00	3,70	2,00	0,90
m	20	111,71	44145,00	52242,00	1,03	632,44	618,00	24,00	7,00	1,20	0,90
M	21	114,95	24581,00	47009,00	1,20	650,78	643,00	54,00	3,90	1,10	8,30
m	22	117,63	3700,00	50752,00	1,20	665,91	643,00	54,00	0,59	4,80	8,30
m	23	121,37	1178,00	42266,00	1,21	687,05	643,00	54,00	0,19	13,60	8,30
	24	127,75	2133,00	34434,00	1,06	723,16	715,00	18,00	0,34	15,90	0,00
M	25	133,96	1018,00	32442,00	0,99	758,29	750,00	45,00	0,16	14,00	1,50
m	26	135,79	4018,00	34653,00	1,00	768,61	750,00	45,00	0,64	4,30	1,50
m	27	138,51	1676,00	35078,00	1,00	783,98	750,00	45,00	0,27	9,00	1,50
	28	144,01	506,00	26641,00	0,51	815,13	809,00	14,00	0,08	53,70	0,00
M	29	148,56	679,00	29533,00	1,00	840,85	834,00	47,00	0,11	21,60	0,90
m	30	150,09	36701,00	35332,00	1,01	849,48	834,00	47,00	5,80	0,70	0,90
m	31	151,54	7613,00	33757,00	1,01	857,68	834,00	47,00	1,20	2,20	0,90
m	32	154,18	1664,00	32145,00	1,01	872,61	834,00	47,00	0,26	8,80	0,90
M	33	163,85	866,00	32564,00	1,04	927,28	919,00	52,00	0,14	16,30	1,30
m	34	166,23	29108,00	33483,00	1,04	940,78	919,00	52,00	4,60	0,80	1,30
m	35	169,26	5062,00	30625,00	1,04	957,92	919,00	52,00	0,80	3,00	1,30
M	36	181,25	20954,00	31139,00	1,03	1025,68	1013,00	113,00	3,30	1,00	0,90
m	37	182,65	5437,00	30893,00	1,03	1033,61	1013,00	113,00	0,86	3,30	0,90
m	38	184,51	923,00	29044,00	1,03	1044,12	1013,00	113,00	0,15	10,80	0,90
m	39	186,12	3007,00	30468,00	1,04	1053,22	1013,00	113,00	0,48	3,70	0,90
m	40	188,89	633,00	28584,00	1,04	1068,93	1013,00	113,00	0,10	13,40	0,90
m	41	190,67	18200,00	28295,00	1,04	1078,95	1013,00	113,00	2,90	1,40	0,90
m	42	192,32	6937,00	29550,00	1,04	1088,30	1013,00	113,00	1,10	2,10	0,90
m	43	193,91	714,00	29351,00	1,05	1097,31	1013,00	113,00	0,11	20,60	0,90
m	44	196,63	11006,00	29046,00	1,05	1112,70	1013,00	113,00	1,70	1,60	0,90
	45	201,60	9344,00	32169,00	1,04	1140,79	1133,00	22,00	1,50	3,90	0,00



	Pk	Energy	Area	Bkgnd	FWHM	Channel	Left	PW	Cts/Sec	%err	Fit
M	46	210,77	32514,00	32126,00	1,31	1192,63	1174,00	50,00	5,20	1,50	2,00
m	47	211,98	2843,00	31635,00	1,31	1199,49	1174,00	50,00	0,45	14,10	2,00
m	48	213,83	1709,00	32440,00	1,31	1209,96	1174,00	50,00	0,27	8,50	2,00
M	49	218,61	3807,00	26683,00	1,10	1237,00	1226,00	35,00	0,60	4,10	0,60
m	50	220,86	1296,00	26716,00	1,11	1249,73	1226,00	35,00	0,21	9,90	0,60
M	51	225,59	627,00	22719,00	1,11	1276,47	1269,00	51,00	0,10	20,00	1,40
m	52	228,46	19539,00	26321,00	1,12	1292,71	1269,00	51,00	3,10	1,00	1,40
m	53	231,94	2222,00	23291,00	1,12	1312,34	1269,00	51,00	0,35	5,90	1,40
	54	235,86	2191,00	25169,00	0,99	1334,52	1327,00	20,00	0,35	13,70	0,00
	55	242,27	3998,00	34196,00	1,68	1370,81	1357,00	28,00	0,64	9,90	0,00
	56	250,12	4880,00	28394,00	1,19	1415,20	1402,00	24,00	0,78	7,10	0,00
M	57	255,61	4192,00	22165,00	1,07	1446,23	1435,00	115,00	0,67	3,20	1,10
m	58	258,68	15077,00	21969,00	1,07	1463,57	1435,00	115,00	2,40	1,40	1,10
m	59	260,10	967,00	21867,00	1,08	1471,64	1435,00	115,00	0,15	16,50	1,10
m	60	261,90	4064,00	21762,00	1,08	1481,81	1435,00	115,00	0,65	3,10	1,10
m	61	264,76	1453,00	22749,00	1,08	1497,96	1435,00	115,00	0,23	10,00	1,10
m	62	267,32	1446,00	21490,00	1,08	1512,47	1435,00	115,00	0,23	8,80	1,10
m	63	270,41	1237,00	22469,00	1,09	1529,94	1435,00	115,00	0,20	10,30	1,10
	64	277,93	49831,00	29870,00	1,47	1572,48	1559,00	28,00	7,90	0,90	0,00
M	65	285,83	1302,00	20557,00	1,10	1617,11	1607,00	36,00	0,21	9,80	0,90
m	66	288,69	808,00	20034,00	1,10	1633,30	1607,00	36,00	0,13	14,30	0,90
M	67	293,55	2840,00	17760,00	1,21	1660,81	1653,00	32,00	0,45	4,70	1,20
m	68	295,90	804,00	20483,00	1,21	1674,07	1653,00	32,00	0,13	13,70	1,20
M	69	303,49	1586,00	18926,00	1,14	1717,02	1705,00	112,00	0,25	11,70	2,70
m	70	304,55	11133,00	18789,00	1,15	1723,00	1705,00	112,00	1,80	1,90	2,70
m	71	307,13	63082,00	18951,00	1,15	1737,57	1705,00	112,00	10,00	0,50	2,70
m	72	309,09	517,00	18345,00	1,15	1748,69	1705,00	112,00	0,08	24,30	2,70



	Pk	Energy	Area	Bkgnd	FWHM	Channel	Left	PW	Cts/Sec	%err	Fit
m	73	312,32	17464,00	17090,00	1,15	1766,92	1705,00	112,00	2,80	1,00	2,70
m	74	314,60	5464,00	16780,00	1,16	1779,84	1705,00	112,00	0,87	2,20	2,70
m	75	316,88	8375,00	17352,00	1,16	1792,72	1705,00	112,00	1,30	1,60	2,70
m	76	319,94	287,00	13828,00	1,16	1810,03	1705,00	112,00	0,05	35,20	2,70
M	77	331,37	3182,00	15279,00	1,06	1874,69	1865,00	45,00	0,51	3,60	0,90
m	78	334,48	6534,00	14583,00	1,07	1892,27	1865,00	45,00	1,00	2,80	0,90
m	79	335,61	955,00	14332,00	1,07	1898,67	1865,00	45,00	0,15	14,50	0,90
	80	343,91	6064,00	22044,00	1,34	1945,60	1930,00	29,00	0,96	5,40	0,00
M	81	356,87	1542,00	14974,00	1,18	2018,86	2008,00	33,00	0,25	10,20	1,50
m	82	358,13	11348,00	14816,00	1,18	2026,03	2008,00	33,00	1,80	1,90	1,50
M	83	362,50	825,00	15257,00	1,27	2050,72	2040,00	34,00	0,13	12,30	0,50
m	84	364,26	1249,00	15955,00	1,27	2060,67	2040,00	34,00	0,20	8,90	0,50
	85	373,68	415,00	12428,00	1,11	2113,94	2106,00	19,00	0,07	49,60	0,00
	86	381,79	514,00	12575,00	0,78	2159,79	2150,00	19,00	0,08	40,40	0,00
	87	396,69	1535,00	24243,00	1,19	2244,06	2217,00	38,00	0,24	24,50	0,00
M	88	402,77	12865,00	13697,00	1,20	2278,46	2263,00	63,00	2,00	1,20	1,60
m	89	405,67	5463,00	14350,00	1,20	2294,88	2263,00	63,00	0,87	2,20	1,60
m	90	407,84	4817,00	14350,00	1,21	2307,11	2263,00	63,00	0,77	3,00	1,60
m	91	409,07	3886,00	14350,00	1,21	2314,07	2263,00	63,00	0,62	3,70	1,60
M	92	417,90	677,00	14484,00	1,76	2364,03	2355,00	60,00	0,11	16,10	1,80
m	93	421,71	468,00	18426,00	1,76	2385,54	2355,00	60,00	0,07	22,20	1,80
m	94	424,68	1095,00	16423,00	1,76	2402,34	2355,00	60,00	0,17	10,80	1,80
M	95	430,64	1896,00	14335,00	1,41	2436,10	2421,00	57,00	0,30	5,30	1,40
m	96	433,46	4249,00	13629,00	1,41	2451,99	2421,00	57,00	0,67	3,40	1,40
m	97	435,08	17505,00	14064,00	1,41	2461,18	2421,00	57,00	2,80	1,20	1,40
M	98	445,14	814,00	12083,00	1,29	2518,07	2504,00	234,00	0,13	9,50	1,30
m	99	448,39	543,00	12581,00	1,29	2536,47	2504,00	234,00	0,09	16,90	1,30



	Pk	Energy	Area	Bkgnd	FWHM	Channel	Left	PW	Cts/Sec	%err	Fit
m	100	452,47	9263,00	12497,00	1,29	2559,53	2504,00	234,00	1,50	2,50	1,30
m	101	454,02	3001,00	12435,00	1,29	2568,27	2504,00	234,00	0,48	3,50	1,30
m	102	457,62	658,00	12337,00	1,29	2588,66	2504,00	234,00	0,10	7,90	1,30
m	103	458,89	2145,00	12314,00	1,30	2595,83	2504,00	234,00	0,34	11,10	1,30
m	104	461,13	7574,00	12252,00	1,30	2608,48	2504,00	234,00	1,20	2,00	1,30
m	105	462,86	7601,00	12166,00	1,30	2618,30	2504,00	234,00	1,20	2,40	1,30
m	106	464,80	5615,00	12080,00	1,30	2629,27	2504,00	234,00	0,89	4,20	1,30
m	107	467,38	2282,00	12027,00	1,30	2643,82	2504,00	234,00	0,36	4,60	1,30
m	108	469,05	430,00	11996,00	1,30	2653,29	2504,00	234,00	0,07	9,60	1,30
m	109	482,38	1390,00	10782,00	1,31	2728,70	2504,00	234,00	0,22	7,20	1,30
M	110	486,98	627,00	10107,00	1,39	2754,68	2746,00	53,00	0,10	14,10	0,80
m	111	488,85	1193,00	11963,00	1,39	2765,25	2746,00	53,00	0,19	8,00	0,80
m	112	492,68	1734,00	11327,00	1,40	2786,92	2746,00	53,00	0,28	5,90	0,80
	113	505,98	1523,00	11345,00	1,20	2862,16	2852,00	23,00	0,24	14,00	0,00
M	114	511,02	2281,00	17375,00	2,20	2890,64	2876,00	51,00	0,36	5,30	1,40
m	115	514,44	1685,00	12658,00	1,48	2909,98	2876,00	51,00	0,27	6,10	1,40
M	116	526,60	3053,00	11513,00	1,42	2978,77	2962,00	53,00	0,48	3,40	1,10
m	117	530,09	5901,00	11787,00	1,42	2998,47	2962,00	53,00	0,94	2,10	1,10
	118	535,08	1024,00	10693,00	1,17	3026,73	3015,00	22,00	0,16	19,80	0,00
M	119	540,81	5487,00	10326,00	1,34	3059,12	3048,00	79,00	0,87	2,10	0,60
m	120	545,09	3290,00	10716,00	1,35	3083,34	3048,00	79,00	0,52	3,10	0,60
m	121	546,90	8258,00	10235,00	1,35	3093,55	3048,00	79,00	1,30	1,60	0,60
m	122	550,91	1369,00	10180,00	1,35	3116,23	3048,00	79,00	0,22	6,40	0,60
	123	555,59	5279,00	13323,00	1,40	3142,67	3129,00	31,00	0,84	5,00	0,00
	124	566,08	9440,00	11300,00	1,39	3202,04	3189,00	26,00	1,50	2,50	0,00
M	125	574,19	395,00	8605,00	1,21	3247,86	3239,00	41,00	0,06	19,30	1,10
m	126	578,00	1222,00	8910,00	1,21	3269,44	3239,00	41,00	0,19	7,60	1,10



	Pk	Energy	Area	Bkgnd	FWHM	Channel	Left	PW	Cts/Sec	%err	Fit
	127	590,62	5471,00	10458,00	1,60	3340,81	3330,00	25,00	0,87	4,00	0,00
	128	595,38	6540,00	10658,00	1,34	3367,70	3355,00	26,00	1,00	3,50	0,00
M	129	602,00	1658,00	8543,00	1,15	3405,14	3387,00	70,00	0,26	5,70	1,20
m	130	604,95	258,00	8462,00	1,15	3421,84	3387,00	70,00	0,04	27,30	1,20
m	131	608,38	235,00	8797,00	1,15	3441,26	3387,00	70,00	0,04	30,50	1,20
M	132	620,16	667,00	10144,00	1,38	3507,85	3495,00	85,00	0,11	16,30	0,90
m	133	621,75	6471,00	10192,00	1,38	3516,83	3495,00	85,00	1,00	2,40	0,90
m	134	625,20	843,00	10710,00	1,39	3536,35	3495,00	85,00	0,13	9,70	0,90
m	135	627,88	1406,00	10769,00	1,39	3551,50	3495,00	85,00	0,22	6,20	0,90
m	136	630,97	722,00	9968,00	1,39	3568,96	3495,00	85,00	0,11	11,70	0,90
	137	636,39	1258,00	8559,00	1,46	3599,63	3591,00	21,00	0,20	14,30	0,00
M	138	641,22	21221,00	10499,00	1,43	3626,95	3613,00	63,00	3,40	1,30	0,80
m	139	642,58	2161,00	10111,00	1,44	3634,64	3613,00	63,00	0,34	10,10	0,80
m	140	645,36	640,00	10131,00	1,44	3650,40	3613,00	63,00	0,10	12,90	0,80
m	141	647,49	6020,00	10143,00	1,44	3662,42	3613,00	63,00	0,96	1,90	0,80
M	142	652,85	642,00	9414,00	1,29	3692,75	3681,00	75,00	0,10	13,20	1,50
m	143	654,36	963,00	9410,00	1,29	3701,27	3681,00	75,00	0,15	9,00	1,50
m	144	657,97	4969,00	9400,00	1,30	3721,67	3681,00	75,00	0,79	2,20	1,50
m	145	662,16	1187,00	8980,00	1,30	3745,39	3681,00	75,00	0,19	7,00	1,50
	146	668,09	764,00	7638,00	0,25	3778,93	3770,00	21,00	0,12	22,10	0,00
M	147	677,19	4400,00	9340,00	1,45	3830,39	3813,00	45,00	0,70	2,50	1,10
m	148	680,40	449,00	8050,00	1,45	3848,54	3813,00	45,00	0,07	17,00	1,10
	149	695,54	773,00	7550,00	1,23	3934,13	3923,00	22,00	0,12	22,10	0,00
M	150	710,19	802,00	7137,00	1,50	4016,99	4007,00	44,00	0,13	9,40	0,90
m	151	712,89	2220,00	8390,00	1,50	4032,28	4007,00	44,00	0,35	4,20	0,90
M	152	719,68	998,00	8078,00	1,89	4070,65	4061,00	43,00	0,16	8,50	1,90
m	153	723,77	1873,00	8360,00	1,90	4093,79	4061,00	43,00	0,30	5,10	1,90



	Pk	Energy	Area	Bkgnd	FWHM	Channel	Left	PW	Cts/Sec	%err	Fit
M	154	731,10	1119,00	8251,00	1,69	4135,24	4122,00	96,00	0,18	7,10	1,30
m	155	735,60	1658,00	8621,00	1,69	4160,69	4122,00	96,00	0,26	4,90	1,30
m	156	739,02	1518,00	8449,00	1,69	4180,06	4122,00	96,00	0,24	5,30	1,30
m	157	742,83	13189,00	7851,00	1,70	4201,61	4122,00	96,00	2,10	1,10	1,30
M	158	748,05	794,00	6102,00	1,36	4231,12	4220,00	54,00	0,13	9,60	1,20
m	159	749,62	1773,00	6448,00	1,36	4239,96	4220,00	54,00	0,28	5,00	1,20
m	160	753,56	1634,00	6648,00	1,36	4262,29	4220,00	54,00	0,26	4,90	1,20
	161	759,83	335,00	5018,00	0,55	4297,73	4289,00	20,00	0,05	39,90	0,00
	162	767,06	14290,00	9022,00	1,55	4338,63	4320,00	36,00	2,30	1,80	0,00
M	163	786,78	1163,00	5597,00	1,47	4450,15	4438,00	61,00	0,18	6,00	1,10
m	164	788,84	1390,00	6033,00	1,48	4461,77	4438,00	61,00	0,22	5,20	1,10
m	165	793,26	2520,00	6239,00	1,48	4486,76	4438,00	61,00	0,40	3,40	1,10
M	166	812,80	1692,00	5820,00	1,60	4597,28	4582,00	62,00	0,27	4,50	1,00
m	167	815,95	581,00	5699,00	1,60	4615,12	4582,00	62,00	0,09	10,70	1,00
m	168	818,98	1303,00	5197,00	1,61	4632,25	4582,00	62,00	0,21	5,50	1,00
M	169	834,72	1123,00	5741,00	1,57	4721,26	4710,00	99,00	0,18	6,70	1,40
m	170	836,71	581,00	6143,00	1,57	4732,53	4710,00	99,00	0,09	12,10	1,40
m	171	839,37	2365,00	6048,00	1,58	4747,53	4710,00	99,00	0,38	3,40	1,40
m	172	843,97	2767,00	5871,00	1,58	4773,57	4710,00	99,00	0,44	2,90	1,40
m	173	846,84	42525,00	5568,00	1,58	4789,82	4710,00	99,00	6,80	0,50	1,40
M	174	857,16	2421,00	5120,00	1,41	4848,17	4837,00	61,00	0,38	3,30	1,70
m	175	861,79	300,00	4965,00	1,41	4874,36	4837,00	61,00	0,05	19,30	1,70
m	176	863,73	2569,00	4778,00	1,42	4885,29	4837,00	61,00	0,41	3,20	1,70
M	177	871,46	2442,00	5297,00	1,71	4929,01	4914,00	58,00	0,39	3,30	1,60
m	178	876,02	1618,00	5176,00	1,72	4954,84	4914,00	58,00	0,26	4,40	1,60
M	179	881,39	2532,00	4628,00	1,60	4985,20	4972,00	122,00	0,40	3,10	1,00
m	180	883,91	28616,00	4800,00	1,60	4999,43	4972,00	122,00	4,50	0,60	1,00



	Pk	Energy	Area	Bkgnd	FWHM	Channel	Left	PW	Cts/Sec	%err	Fit
m	181	888,30	971,00	4445,00	1,60	5024,28	4972,00	122,00	0,15	5,80	1,00
m	182	892,49	688,00	4393,00	1,60	5047,98	4972,00	122,00	0,11	9,10	1,00
m	183	894,71	3288,00	4512,00	1,61	5060,49	4972,00	122,00	0,52	2,40	1,00
m	184	897,79	1698,00	4303,00	1,61	5077,94	4972,00	122,00	0,27	3,90	1,00
M	185	912,42	9135,00	4366,00	1,53	5160,65	5142,00	70,00	1,50	1,30	1,10
m	186	914,46	1961,00	4492,00	1,53	5172,19	5142,00	70,00	0,31	3,80	1,10
m	187	918,58	9558,00	4691,00	1,54	5195,48	5142,00	70,00	1,50	1,20	1,10
	188	925,45	507,00	3458,00	0,76	5234,36	5227,00	20,00	0,08	22,20	0,00
M	189	932,60	1985,00	4753,00	1,76	5274,79	5259,00	41,00	0,32	4,80	1,20
m	190	934,33	1611,00	4529,00	1,76	5284,55	5259,00	41,00	0,26	5,60	1,20
M	191	943,12	4101,00	4722,00	1,91	5334,29	5318,00	60,00	0,65	2,10	2,00
m	192	947,81	3651,00	4710,00	1,91	5360,81	5318,00	60,00	0,58	2,30	2,00
	193	953,31	1821,00	4835,00	1,67	5391,90	5377,00	35,00	0,29	9,20	0,00
	194	963,89	282,00	3234,00	0,46	5451,72	5442,00	21,00	0,05	38,90	0,00
M	195	974,49	1659,00	3960,00	1,59	5511,71	5492,00	57,00	0,26	4,10	1,10
m	196	978,04	787,00	3900,00	1,59	5531,75	5492,00	57,00	0,13	7,20	1,10
M	197	996,89	579,00	3974,00	1,78	5638,38	5624,00	55,00	0,09	9,60	0,90
m	198	1000,64	1488,00	4057,00	1,78	5659,60	5624,00	55,00	0,24	4,60	0,90
M	199	1009,49	11840,00	4199,00	1,75	5709,62	5689,00	76,00	1,90	1,10	1,30
m	200	1012,06	1791,00	4164,00	1,75	5724,16	5689,00	76,00	0,28	3,90	1,30
m	201	1016,47	363,00	4141,00	1,76	5749,11	5689,00	76,00	0,06	14,60	1,30
	202	1024,10	1794,00	3190,00	1,44	5792,26	5783,00	22,00	0,29	6,50	0,00
	203	1031,72	6631,00	4338,00	1,75	5835,35	5818,00	34,00	1,10	2,60	0,00
M	204	1039,32	1419,00	4380,00	2,29	5878,30	5863,00	53,00	0,23	5,10	1,30
m	205	1043,44	641,00	4156,00	2,30	5901,59	5863,00	53,00	0,10	9,40	1,30
	206	1061,58	284,00	3134,00	0,77	6004,19	5990,00	27,00	0,05	41,70	0,00
	207	1072,41	5186,00	4018,00	1,67	6065,44	6048,00	35,00	0,82	3,20	0,00



	Pk	Energy	Area	Bkgnd	FWHM	Channel	Left	PW	Cts/Sec	%err	Fit
	208	1078,47	876,00	3800,00	1,68	6099,71	6082,00	32,00	0,14	16,10	0,00
	209	1093,96	436,00	3263,00	0,45	6187,33	6173,00	29,00	0,07	28,60	0,00
	210	1103,50	230,00	3057,00	0,18	6241,27	6231,00	25,00	0,04	49,20	0,00
	211	1123,29	943,00	4600,00	1,06	6353,20	6336,00	38,00	0,15	17,60	0,00
M	212	1131,42	1930,00	3757,00	1,76	6399,15	6378,00	130,00	0,31	3,50	1,00
m	213	1136,11	3316,00	3706,00	1,76	6425,69	6378,00	130,00	0,53	2,40	1,00
m	214	1138,86	653,00	3673,00	1,76	6441,24	6378,00	130,00	0,10	8,00	1,00
m	215	1141,97	736,00	3648,00	1,76	6458,85	6378,00	130,00	0,12	7,50	1,00
m	216	1147,04	1233,00	3608,00	1,76	6487,53	6378,00	130,00	0,20	4,80	1,00
	217	1153,06	150,00	2011,00	0,32	6521,56	6513,00	18,00	0,02	54,90	0,00
	218	1160,60	943,00	5009,00	1,55	6564,17	6543,00	40,00	0,15	18,70	0,00
	219	1197,18	328,00	4173,00	0,82	6771,06	6750,00	34,00	0,05	45,40	0,00
	220	1203,98	499,00	3815,00	1,18	6809,52	6794,00	29,00	0,08	27,00	0,00
	221	1233,11	451,00	2538,00	0,32	6974,24	6959,00	27,00	0,07	23,80	0,00
	222	1248,18	3307,00	3452,00	1,64	7059,46	7043,00	32,00	0,53	4,30	0,00
	223	1260,43	2341,00	2717,00	1,70	7128,76	7112,00	31,00	0,37	5,30	0,00
	224	1268,83	295,00	2285,00	0,71	7176,26	7163,00	28,00	0,05	34,90	0,00
	225	1283,44	538,00	2777,00	1,12	7258,90	7237,00	38,00	0,09	23,90	0,00
	226	1304,02	153,00	1368,00	1,06	7375,27	7367,00	19,00	0,02	45,10	0,00
	227	1323,87	631,00	2211,00	1,30	7487,54	7465,00	35,00	0,10	17,70	0,00
	228	1333,35	529,00	1664,00	1,33	7541,13	7530,00	25,00	0,08	16,30	0,00
	229	1355,70	202,00	1558,00	0,32	7667,53	7657,00	25,00	0,03	40,20	0,00
	230	1363,09	461,00	1467,00	1,11	7709,33	7696,00	26,00	0,07	17,80	0,00
	231	1369,87	345,00	1952,00	0,47	7747,70	7729,00	35,00	0,06	30,20	0,00
	232	1376,93	608,00	1929,00	1,35	7787,58	7769,00	32,00	0,10	16,70	0,00
	233	1384,07	13001,00	2585,00	1,81	7827,98	7806,00	43,00	2,10	1,30	0,00
	234	1405,62	128,00	1279,00	0,55	7949,87	7938,00	23,00	0,02	55,50	0,00



	Pk	Energy	Area	Bkgnd	FWHM	Channel	Left	PW	Cts/Sec	%err	Fit
	235	1436,02	20899,00	2087,00	1,94	8121,75	8101,00	41,00	3,30	0,90	0,00
	236	1445,29	225,00	1229,00	1,23	8174,16	8161,00	24,00	0,04	31,90	0,00
M	237	1455,51	453,00	1756,00	1,73	8231,99	8219,00	58,00	0,07	9,20	0,80
m	238	1457,94	615,00	1779,00	1,73	8245,75	8219,00	58,00	0,10	7,10	0,80
m	239	1461,11	236,00	1609,00	1,74	8263,63	8219,00	58,00	0,04	14,90	0,80
	240	1470,40	203,00	1623,00	0,28	8316,20	8302,00	31,00	0,03	44,40	0,00
	241	1516,62	165,00	1283,00	1,04	8577,58	8565,00	26,00	0,03	45,50	0,00
M	242	1525,16	1589,00	1593,00	1,95	8625,90	8611,00	73,00	0,25	3,40	0,90
m	243	1530,24	690,00	1608,00	1,95	8654,63	8611,00	73,00	0,11	6,30	0,90
m	244	1532,89	400,00	1480,00	1,95	8669,57	8611,00	73,00	0,06	9,60	0,90
M	245	1541,96	93,00	1515,00	2,50	8720,89	8711,00	59,00	0,02	31,00	0,90
m	246	1546,58	565,00	1903,00	2,51	8747,03	8711,00	59,00	0,09	7,10	0,90
	247	1614,21	1070,00	1682,00	1,86	9129,49	9107,00	38,00	0,17	9,70	0,00
	248	1672,29	194,00	778,00	0,79	9457,91	9447,00	22,00	0,03	28,80	0,00
M	249	1678,44	693,00	1543,00	2,48	9492,69	9473,00	73,00	0,11	6,30	1,30
m	250	1683,83	490,00	1595,00	2,48	9523,18	9473,00	73,00	0,08	8,10	1,30
	251	1707,49	542,00	1335,00	1,81	9657,03	9633,00	38,00	0,09	16,70	0,00
M	252	1718,12	188,00	998,00	2,56	9717,09	9706,00	60,00	0,03	16,60	0,80
m	253	1723,50	376,00	1223,00	2,56	9747,52	9706,00	60,00	0,06	10,00	0,80
	254	1731,96	200,00	968,00	0,39	9795,39	9783,00	31,00	0,03	35,00	0,00
	255	1742,01	702,00	1274,00	2,20	9852,21	9835,00	37,00	0,11	12,60	0,00
	256	1757,20	427,00	908,00	2,10	9938,10	9924,00	29,00	0,07	16,00	0,00
	257	1768,92	1091,00	1321,00	1,70	10004,40	9984,00	39,00	0,17	8,60	0,00
	258	1792,12	494,00	834,00	0,93	10135,60	10123,00	29,00	0,08	13,40	0,00
	259	1807,62	1278,00	1050,00	1,98	10223,20	10204,00	35,00	0,20	6,50	0,00
	260	1836,97	1244,00	1078,00	1,94	10389,20	10370,00	36,00	0,20	6,80	0,00
M	261	1882,83	120,00	640,00	1,25	10648,6	10631,00	52,00	0,02	20,10	1,10



	Pk	Energy	Area	Bkgnd	FWHM	Channel	Left	PW	Cts/Sec	%err	Fit
m	262	1886,59	88,00	720,00	1,25	10669,8	10631,00	52,00	0,01	27,10	1,10
M	263	1898,93	348,00	989,00	2,13	10739,6	10724,00	54,00	0,06	9,20	1,00
m	264	1902,48	864,00	1040,00	2,13	10759,7	10724,00	54,00	0,14	4,80	1,00
	265	2005,81	686,00	914,00	1,65	11344	11324,00	40,00	0,11	11,50	0,00
	266	2016,98	577,00	928,00	2,14	11407,2	11391,00	32,00	0,09	12,50	0,00
M	267	2032,34	526,00	1154,00	3,32	11494,1	11478,00	55,00	0,08	8,40	1,40
m	268	2036,48	114,00	1126,00	3,32	11517,5	11478,00	55,00	0,02	30,40	1,40
	269	2056,30	231,00	560,00	0,93	11629,6	11615,00	27,00	0,04	22,40	0,00
	270	2101,63	87,00	394,00	0,50	11885,9	11875,00	22,00	0,01	45,50	0,00
	271	2129,69	128,00	549,00	0,31	12044,6	12033,00	28,00	0,02	40,00	0,00
	272	2176,08	176,00	438,00	0,88	12306,9	12295,00	26,00	0,03	25,60	0,00
	273	2188,58	577,00	596,00	2,10	12377,6	12360,00	35,00	0,09	10,70	0,00
	274	2197,34	1360,00	569,00	2,16	12427,2	12408,00	37,00	0,22	5,00	0,00
	275	2219,25	2942,00	616,00	2,30	12551,1	12527,00	46,00	0,47	2,90	0,00
	276	2232,97	218,00	318,00	1,33	12628,7	12616,00	27,00	0,04	18,50	0,00
	277	2253,46	191,00	478,00	0,31	12744,5	12727,00	32,00	0,03	26,60	0,00
M	278	2393,80	1647,00	385,00	2,47	13538,2	13516,00	75,00	0,26	2,70	1,20
m	279	2399,51	1422,00	391,00	2,47	13570,5	13516,00	75,00	0,23	3,00	1,20
	280	2410,31	78,00	177,00	0,26	13631,6	13621,00	23,00	0,01	35,60	0,00
	281	2486,03	129,00	135,00	0,29	14059,8	14049,00	23,00	0,02	19,90	0,00
	282	2544,76	920,00	247,00	2,53	14391,9	14370,00	42,00	0,15	5,40	0,00
	283	2556,67	375,00	241,00	1,50	14459,3	14444,00	29,00	0,06	10,30	0,00
	284	2571,98	446,00	135,00	2,01	14545,9	14530,00	36,00	0,07	7,70	0,00
	285	2616,41	86,00	81,00	0,21	14797,2	14787,00	22,00	0,01	23,10	0,00
	286	2633,58	140,00	84,00	0,21	14894,2	14881,00	27,00	0,02	16,20	0,00
	287	2641,38	1240,00	111,00	2,55	14938,4	14915,00	44,00	0,20	3,60	0,00
	288	2668,88	126,00	112,00	0,39	15093,9	15083,00	24,00	0,02	19,00	0,00



	Pk	Energy	Area	Bkgnd	FWHM	Channel	Left	PW	Cts/Sec	%err	Fit
	289	2679,98	48,00	99,00	0,73	15156,6	15146,00	22,00	0,01	42,40	0,00
	290	2709,14	83,00	78,00	0,73	15321,5	15310,00	24,00	0,01	23,90	0,00
	291	2820,38	47,00	66,00	1,08	15950,6	15939,00	24,00	0,01	37,60	0,00

MEASUREMENT 4

	Pk	IT	Energy	Area	Bkgnd	FWHM	Channel	Left	PW	Cts/Sec	%err	Fit
M	1	32	25,35	42209	8945	0,48	144,02	139	34	1,70E-01	0,6	346,3
m	2	32	25,96	27210	17495	0,48	147,5	139	34	1,10E-01	0,8	346,3
m	3	32	26,55	23340	25978	0,48	150,85	139	34	9,40E-02	0,9	346,3
m	4	32	27,17	22428	36998	0,48	154,36	139	34	9,00E-02	1	346,3
m	5	32	27,84	17219	47916	0,49	158,12	139	34	6,90E-02	1,3	346,3
m	6	32	28,54	13418	63633	0,49	162,08	139	34	5,40E-02	1,7	346,3
M	7	10	61,08	3384	138050	0,94	346,12	335	37	1,40E-02	8,6	2,8
m	8	10	62,36	5875	140104	0,94	353,32	335	37	2,40E-02	5,2	2,8
m	9	10	63,77	215013	144469	0,94	361,34	335	37	8,60E-01	0,3	2,8
M	10	7	81,73	8570	243526	0,98	462,87	451	38	3,40E-02	4,4	2,7
m	11	7	83,66	14111	258896	0,99	473,8	451	38	5,70E-02	3,8	2,7
m	12	7	84,67	40912	252664	0,99	479,5	451	38	1,60E-01	1,6	2,7
M	13	7	90,51	40117	315708	1,1	512,54	499	52	1,60E-01	1,2	67,6
m	14	7	93,05	1340512	349578	1,1	526,89	499	52	5,40E+00	0,1	67,6
m	15	7	95,11	453228	350323	1,11	538,55	499	52	1,80E+00	0,2	67,6
	16	0	98,9	805317	337412	1,02	560,02	550	22	3,20E+00	0,2	0
M	17	32	103,89	5191	301935	1,45	588,22	577	93	2,10E-02	8	59,9
m	18	32	105,96	24540	314308	1,45	599,94	577	93	9,90E-02	1,8	59,9



	Pk	IT	Energy	Area	Bkgnd	FWHM	Channel	Left	PW	Cts/Sec	%err	Fit
m	19	32	107,79	14710	302397	1,46	610,27	577	93	5,90E-02	2,9	59,9
m	20	32	109,72	53563	285254	1,46	621,17	577	93	2,20E-01	0,9	59,9
m	21	32	111,51	366657	261043	1,46	631,31	577	93	1,50E+00	0,2	59,9
m	22	32	113,24	142472	234431	1,47	641,08	577	93	5,70E-01	0,4	59,9
m	23	32	115,11	155551	211685	1,47	651,69	577	93	6,20E-01	0,3	59,9
	24	0	121,27	2697	149530	0,78	686,48	674	20	1,10E-02	26,9	0
	25	0	131,75	6743	143569	1,04	745,77	738	19	2,70E-02	10,4	0
M	26	5	141,26	2675	134604	1,01	799,56	791	48	1,10E-02	10,5	0,8
m	27	5	144,23	90441	132684	1,02	816,32	791	48	3,60E-01	0,5	0,8
m	28	5	145,92	10901	131255	1,02	825,88	791	48	4,40E-02	2,7	0,8
	29	0	153,22	2179	150136	0,28	867,17	859	21	8,70E-03	33,9	0
	30	0	163,78	48997	177546	1,07	926,93	914	26	2,00E-01	1,8	0
M	31	6	183,05	2860	106545	1,04	1035,88	1028	39	1,10E-02	9,3	1,3
m	32	6	186,14	551743	111124	1,05	1053,34	1028	39	2,20E+00	0,1	1,3
	33	0	195,35	4223	80189	0,97	1105,42	1099	15	1,70E-02	11,5	0
M	34	5	202,57	8849	93781	1,07	1146,29	1134	41	3,60E-02	2,8	1,1
m	35	5	205,73	48972	96290	1,08	1164,13	1134	41	2,00E-01	0,7	1,1
	36	0	221,58	755	50582	0,82	1253,8	1248	12	3,00E-03	47,4	0
M	37	23	227,29	3490	87552	1,41	1286,07	1277	37	1,40E-02	17,5	0,9
m	38	23	228,46	1499	98641	1,41	1292,68	1277	37	6,00E-03	35,5	0,9
	39	0	249,67	710	39852	0,61	1412,64	1407	12	2,90E-03	44,7	0
	40	0	258,61	19587	72946	1,11	1463,21	1454	24	7,90E-02	2,9	0
	41	0	305,26	615	34295	0,3	1727,04	1720	16	2,50E-03	52,4	0
	42	0	329,04	3506	43515	1,29	1861,51	1853	24	1,40E-02	12	0
	43	0	352,2	1509	34088	1,09	1992,5	1984	22	6,10E-03	23,9	0
	44	0	364,76	4431	34245	1,14	2063,48	2055	24	1,80E-02	8,5	0
M	45	10	369,83	646	20840	0,89	2092,17	2085	33	2,60E-03	20,1	1,4



	Pk	IT	Energy	Area	Bkgnd	FWHM	Channel	Left	PW	Cts/Sec	%err	Fit
m	46	10	372,21	434	21720	0,89	2105,61	2085	33	1,70E-03	27,3	1,4
	47	0	424,05	367	14403	0,27	2398,8	2392	14	1,50E-03	54,6	0
	48	0	487,19	6085	20451	1,4	2755,9	2744	26	2,40E-02	5	0
	49	0	497,26	6248	20418	1,33	2812,82	2796	27	2,50E-02	4,9	0
	50	0	511,14	6233	26194	2,62	2891,31	2874	34	2,50E-02	6,1	0
	51	0	531,03	510	13714	0,95	3003,82	2994	20	2,00E-03	43,2	0
	52	0	537,42	3257	20623	1,31	3039,96	3026	31	1,30E-02	9,9	0
	53	0	544,12	486	11723	0,4	3077,85	3070	18	2,00E-03	40,5	0
	54	0	569,29	2109	15468	1,43	3220,15	3211	25	8,50E-03	12,2	0
	55	0	583,25	841	12962	0,78	3299,12	3289	23	3,40E-03	26,9	0
	56	0	609,46	1626	11858	1,17	3447,34	3435	23	6,50E-03	13,4	0
	57	0	691,01	1279	10622	1,05	3908,55	3899	28	5,10E-03	17,3	0
M	58	6	698,99	589	8394	1,42	3953,69	3944	67	2,40E-03	13,7	0,8
m	59	6	702,12	952	9457	1,42	3971,37	3944	67	3,80E-03	9	0,8
m	60	6	705,99	771	9350	1,43	3993,24	3944	67	3,10E-03	10,8	0,8
	61	0	724,17	2821	9706	1,36	4096,03	4083	25	1,10E-02	7,3	0
	62	0	733,32	946	8497	1,25	4147,82	4138	23	3,80E-03	19,5	0
M	63	4	739,95	1337	9721	1,53	4185,29	4165	52	5,40E-03	6,3	1,2
m	64	4	742,75	10161	9625	1,54	4201,14	4165	52	4,10E-02	1,3	1,2
	65	0	751,77	275	7458	1,01	4252,12	4240	21	1,10E-03	60,2	0
	66	0	756,69	3896	11000	1,4	4279,98	4263	31	1,60E-02	6,2	0
	67	0	766,3	41634	13442	1,57	4334,32	4315	38	1,70E-01	0,8	0
M	68	5	781,81	1093	9524	1,56	4422,01	4403	61	4,40E-03	7,4	0,9
m	69	5	786,2	5778	9542	1,57	4446,83	4403	61	2,30E-02	2	0,9
	70	0	805,57	1172	8048	1,44	4556,42	4547	29	4,70E-03	16,7	0
M	71	6	815,63	2186	7075	1,53	4613,27	4599	48	8,80E-03	4,1	0,8
m	72	6	819,07	330	6995	1,54	4632,73	4599	48	1,30E-03	20	0,8



	Pk	IT	Energy	Area	Bkgnd	FWHM	Channel	Left	PW	Cts/Sec	%err	Fit
	73	0	824,53	317	6104	0,63	4663,62	4651	23	1,30E-03	48,9	0
	74	0	831,42	500	4939	0,6	4702,59	4693	20	2,00E-03	26,7	0
	75	0	851,54	545	6209	1,3	4816,38	4805	28	2,20E-03	31	0
	76	0	867,57	409	3940	1,97	4907,04	4899	19	1,60E-03	28,7	0
M	77	6	875,82	660	5333	1,75	4953,68	4940	96	2,70E-03	9,7	0,9
m	78	6	880,35	2246	5589	1,76	4979,29	4940	96	9,00E-03	3,5	0,9
m	79	6	883,2	1923	5502	1,76	4995,44	4940	96	7,70E-03	3,9	0,9
m	80	6	887,43	744	5398	1,76	5019,33	4940	96	3,00E-03	8,5	0,9
	81	0	898,57	621	5253	1,1	5082,33	5067	31	2,50E-03	26,1	0
	82	0	911,08	1238	5240	1,26	5153,08	5135	31	5,00E-03	13,2	0
M	83	19	921,51	759	5307	2,35	5212,08	5204	48	3,00E-03	9,1	3
m	84	19	925,77	2838	6396	2,35	5236,15	5204	48	1,10E-02	3,3	3
	85	0	945,83	2902	5007	1,55	5349,6	5335	31	1,20E-02	5,7	0
M	86	5	964,64	289	3367	1,6	5455,99	5447	45	1,20E-03	18,1	1,1
m	87	5	968,79	794	3958	1,6	5479,46	5447	45	3,20E-03	8,1	1,1
	88	0	980,37	354	4116	1,13	5544,93	5525	28	1,40E-03	38,9	0
	89	0	994,86	519	2981	1,04	5626,88	5617	21	2,10E-03	20,5	0
	90	0	1000,91	79713	5124	1,66	5661,11	5641	40	3,20E-01	0,4	0
	91	0	1044,61	214	2512	0,35	5908,22	5897	22	8,60E-04	45,9	0
M	92	12	1120,28	1216	3383	2,25	6336,15	6319	64	4,90E-03	5,2	1,3
m	93	12	1125,19	678	3356	2,26	6363,94	6319	64	2,70E-03	7,9	1,3
	94	0	1193,87	937	2852	1,63	6752,32	6739	30	3,80E-03	12,9	0
	95	0	1237,92	809	2989	1,45	7001,46	6985	34	3,20E-03	15,9	0
	96	0	1377,81	254	1343	0,78	7792,58	7781	25	1,00E-03	29,9	0
	97	0	1394,15	247	1327	0,25	7884,98	7874	27	9,90E-04	31,5	0
M	98	8	1408,3	306	1897	2,39	7964,98	7945	73	1,20E-03	13,6	0,8
m	99	8	1414,28	243	1774	2,39	7998,82	7945	73	9,80E-04	16	0,8



	Pk	IT	Energy	Area	Bkgnd	FWHM	Channel	Left	PW	Cts/Sec	%err	Fit
	100	0	1434,52	555	1485	1,36	8113,3	8100	30	2,20E-03	15,7	0
	101	0	1461,22	16590	1778	1,93	8264,27	8241	43	6,70E-02	1	0
M	102	8	1510,55	1091	1144	2,33	8543,27	8520	50	4,40E-03	4,7	1
m	103	8	1513,54	108	776	2,33	8560,15	8520	50	4,30E-04	30,4	1
	104	0	1554,38	444	977	1,05	8791,11	8773	34	1,80E-03	16,8	0
	105	0	1596,82	4146	1776	1,91	9031,11	9013	41	1,70E-02	2,9	0
	106	0	1631,12	142	540	0,39	9225,11	9212	25	5,70E-04	34,5	0
	107	0	1730,33	297	451	2,02	9786,15	9775	26	1,20E-03	15,9	0
	108	0	1738,59	1201	640	2,22	9832,86	9814	40	4,80E-03	5,9	0
	109	0	1765,59	1832	721	2,25	9985,57	9967	43	7,40E-03	4,4	0
	110	0	1810,23	126	430	0,24	10238	10224	27	5,00E-04	35,7	0
	111	0	1832,34	817	567	2,18	10363	10345	36	3,30E-03	7,7	0
	112	0	1848,52	139	444	0,49	10454,5	10443	29	5,60E-04	33,6	0
	113	0	1868,65	636	389	1,65	10568,4	10551	35	2,60E-03	8,2	0
	114	0	1875,98	517	570	2,01	10609,8	10593	40	2,10E-03	12,2	0
	115	0	1895,05	55	306	0,58	10717,7	10708	20	2,20E-04	61,2	0
	116	0	1912,52	273	463	0,72	10816,4	10799	34	1,10E-03	19,1	0
	117	0	1938,3	125	392	0,67	10962,2	10949	30	5,00E-04	35,6	0
	118	0	2084,5	67	258	0,34	11789	11779	22	2,70E-04	48,1	0
	119	0	2104,88	445	435	2,45	11904,3	11885	40	1,80E-03	12,4	0
	120	0	2119,82	59	252	0,38	11988,8	11978	23	2,40E-04	54,2	0
	121	0	2205,57	400	361	1,81	12473,7	12458	33	1,60E-03	11,9	0
	122	0	2450,01	146	138	0,48	13856,1	13846	23	5,90E-04	17,8	0
	123	0	2523,45	80	121	0,41	14271,5	14261	22	3,20E-04	28,9	0
	124	0	2616,73	3390	131	2,68	14798,9	14775	48	1,40E-02	1,9	0

